

Reviewers' comments are in black, authors' response in blue and changes to the text in red.

## Reviewer #1

### General comments

This is a well-written manuscript describing an important new instrument for quantifying atmospheric isoprene mixing ratios. In light of recent developments in remote sensing of isoprene (e.g. Fu et al. 2019), the need for a low-cost, field deployable measurement of isoprene for satellite verification has become essential. This should be published after minor revision, as described below.

We thank the reviewer for their valuable feedback on the manuscript. Below we address the individual points raised by the reviewer.

Throughout the manuscript, the authors employ a quadratic calibration curve for the instrument without sufficient discussion of the physical cause of the non-linearity, especially as they present curves with both positive and negative coefficients for the 2<sup>nd</sup> order component of the equation (see Fig 16). In light of the overall uncertainties associated with this measurement, it would be enlightening to understand if the non-linearity is statistically significant or if a linear function would be adequate here.

We investigated the impact of using linear or quadratic calibration curves on the isoprene mixing ratios in the sample runs, and found only minor differences (< 1%). This is because the 2<sup>nd</sup> degree coefficient (i.e., the curvature) is effectively very small, and all the sample measurements presented here fall within the dynamic range of the calibration plots (i.e., all determined by interpolation and not extrapolation). The calibration lines in Figure 16 gave an exaggerated idea of the curvature as they effectively extrapolated beyond the highest calibration point (i.e., outside the dynamic range of both calibration and sample runs). We have also amended the x-axis in Figure 16 to reflect this.

Upon closer inspection we found that the statistical significance of the curvature is small even without taking into account the uncertainty in the measurements (i.e., just from the scatter of the points in the calibration plots), and is indeed negligible once the measurement uncertainty (~10%) is taken into account. We also found that, by varying the length of the time interval over which calibration runs are used to produce a calibration plot (typically 1 week; in this test varied between 4 to 10 days), the sign of the curvature of the calibration plot that would be applied to a few selected sample chromatograms changed sign. We conclude that the curvature itself is not an inherent feature of the instrument over the calibrant mass used and that the sign of the curvature is predominantly determined by the number of calibration points at high volumes, as this varies from calibration plot to calibration plot. We agree that a linear fit is better suited to these plots and have amended the plots and text accordingly.

What is conspicuously absent from the manuscript is a figure showing 1) a chromatogram for ambient air, to allow the reader to evaluate the validity of the peak area fitting algorithm in "real" sampling conditions and 2) an intercomparison with a well-established instrument / method for isoprene to evaluate the technique for artefact in measurement of ambient air [e.g. Barket et al., 2001]. This prevents the reader from being able to determine if the signal

response of the instrument in ambient air is responding only to isoprene; because of this, the accuracy of the instrument measurement is not well demonstrated.

In response to point 1), we now present a calibration, a sample and a blank chromatogram with peak fit in the revised Figure 3.

We agree with the reviewer regarding point 2). We are attempting to arrange an intercomparison with a more established instrument for isoprene monitoring under ambient conditions. We have added a sentence to address this point in the Conclusions section to reflect this:

An intercomparison in real ambient air with more established VOC monitoring instrumentation (such as that described by Barkot et al. (2001)) will also help to better evaluate the accuracy of the iDirac.

The underlying data presented here appears to be sufficient for the authors to provide at least two quantitative assessments of the system accuracy that are missing:

1. The diurnal profiles of isoprene shown in Figures 14 and 15 show very low observed mixing ratios for isoprene at night, indicating that species with long atmospheric lifetime relative to isoprene do not present a significant source of interference. Some statistical evaluation of the night-time / pre-dawn data may provide some bound for this potential interference to the method presented.

Assuming there are long-lived co-eluters that are trapped with the same efficiency and have the same PID response as isoprene, the night-time observed concentrations attributed to isoprene could be thought of as an upper limit to this type of interference. We calculated the mean night-time isoprene mixing ratio from the plots in Figures 14 and 15 as 50 ppt in both cases. We have added the following paragraph at the end of the subsection on accuracy in Section 4.2:

“Co-elution of interfering species can also affect accuracy. Tests targeting specific potential interferents are described in Section 5.1 and show that these species do not overlap with the isoprene peak in the chromatograms. However co-elution with unknown (or not tested for) species, albeit unlikely, can never be fully ruled out. If these species have longer lifetimes than isoprene, the observed night-time abundances attributed to isoprene can be used as the upper limit of potential interference of unknown co-eluters (assuming they are trapped with the same efficiency and have the same PID response as isoprene). The isoprene night-time mixing ratio is 50 ppt for the data shown in both Figures 14 and 15. Therefore we estimate the instrument accuracy for field data as the combination of the propagated uncertainty from the standard (10-12.5 %) and the potential co-elution of long-lived species (50 ppt). This correspond to an overall accuracy of  $\pm 1.2$  ppb for a 10 ppb isoprene sample,  $\pm 0.13$  ppb for a 1 ppb isoprene sample and  $\pm 51$  ppt for a 100 ppt isoprene sample.”

2. The peak-fitting technique used to determine isoprene peak area should also provide additional information, such as the fitted peak width (FWHM) and uncertainty of the peak fit area calculation. These can be used to assess the quality of the chromatographic peak, both to evaluate for co-eluters and to account for bias from changes in peak shape (e.g. tailing).

We monitor peak features throughout our analysis routine and have added the following sentence to the end of the co-elution section to address this point:

“Peak width and RMSE from the Gaussian fit, retrieved from the fitting routine described in Section 3.3, can also be used to evaluate the presence of co-eluting species. An additional

peak overlapping to some degree with the target isoprene peak in a sample run would cause a change in the peak shape. This would result in values for the fitted peak width and RMSE that are different from those from the calibration runs. For this reason, we use the width and RMSE from the calibration runs to define a range of acceptable peak widths and RMSE (equal to the mean value  $\pm$  1 standard deviation). Any peaks from sample runs exceeding this range are flagged up for further analysis.”

Some of the technical discussion and the number of figures seems excessive for the manuscript, and the authors should consider creating a supplemental information addendum to the main manuscript to move some of this material (see below for specific suggestions).

### Specific comments

**P1, Line 23. Introduction.** As noted above, a recent publication [Fu et al. 2019] describes isoprene retrieval from space based observation. The uncertainties for this method are typically 10-50%, and therefore the iDirac instrument may provide a suitable means to calibrate the satellite measurement. The above reference serves as a useful basis for defining acceptable uncertainties for an isoprene measurement, and the authors are encouraged to cite it in the introduction.

We added a paragraph to the introduction, reading as follows:

Recent work showed that it is possible to retrieve isoprene abundances in the boundary layer using satellite measurements by means of thermal infra-red imaging (Fu et al., 2019). However, with uncertainties in the range of 10-50%, these retrievals would benefit from further validation from ground-based instrumentation.

**P4, Line 12. Figure 2.** The iDirac plumbing schematic shows the sample trap as a black line between two numbers ports on the Valco valve. This resembles a valve “jumper” – a short piece of tubing connecting two ports – that is the typical convention, and can lead to some confusion. The authors should draw the sample trap as a separate device outside of the valve to make the figure clearer.

Amended.

**P5, line 9. “the trap is flash-heated to approximately 300 °C”** There is no description of how this temperature is measured. Please describe the temp sensor and sensor location relative to the trap adsorbent.

The trap temperature is measured routinely in the lab but not in the field. We found the temperature varied by  $\pm$  5°C. We have added this to the text.

**P5, line 12. “large bulky molecules”** Either “large” or “bulky” is sufficient here.

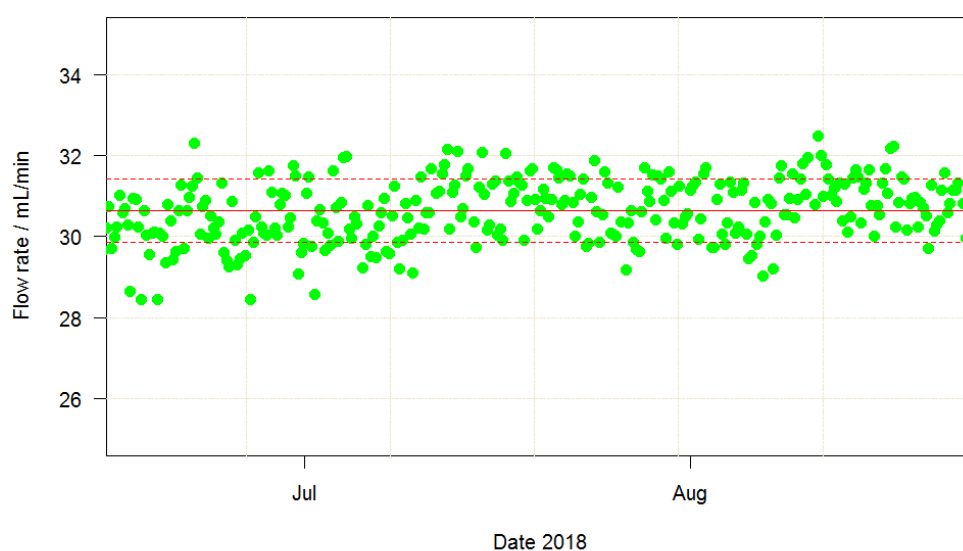
Amended.

**P5, line 38. “a coiled nichrome wire heating element surrounding the section of the [stainless-steel] tube”** Is the heating element in contact with the trap tubing? It would seem that the heater would short across the trap if it is in contact. Can the authors describe how (or if) this is avoided?

The nichrome wire has a ceramic electrically insulating coating to prevent shorting with the trap tubing. We have added a sentence to the text to reflect this.

**P5, line 29. “Flow restrictors upstream from valves 3, 4, 6 and 7”** The authors use small diameter tubing (0.005” ID and 0.0035” ID) rather than critical orifices to restrict reagent gas flow. Can they provide any comment on the long-term performance of this method? This reviewer uses critical orifices in this situation, which have been found to require occasional servicing.

We found good performance in flow regulation over time. Naturally the flow rate downstream of the restrictors is proportional to the gas pressure upstream of the restrictors. However, if the upstream pressure is not changed, we found very little variation in the flow rate. For instance, the plot below shows the flow rate of the calibration gas (valve 3) across a 2-month period in the WIsDOM campaign (described in Section 5.3) during which the regulated output pressure of the calibration cylinder was not changed. The flow (green points) remained stable, within 2.5% (dashed red lines, corresponding to 1 standard deviation) from the average (solid red line).



**P5, line 39. “Carboxen 1016”** I believe the manufacturer has renamed this adsorbent to Graphsphere 2016.

Amended.

**P6, line 5. “heated to 40 °C”** Can the authors provide any statistical description of the actual temperature stability of the oven? Peak retention time is directly related to this temperature, and therefore this is a critical variable in the instrument.

The oven temperature exhibits diurnal variations (typically,  $\pm 2$  °C) that appear driven by ambient temperature. This in turn affects the isoprene retention time. However, with frequent calibrations (every 5 hours) it is possible to track how the retention time changes with time. We found that interpolating between the elution times from two adjacent calibration runs was sufficient to determine the elution time in the sample runs in between. When calibration runs are more infrequent, we derive a linear relationship between oven temperature and isoprene retention time from the calibration runs to constrain the range over which the algorithm fits a Gaussian in the sample runs.

We have added the following sentence to Section 2.1:

“The oven temperature exhibits diurnal variations (typically in the range of  $\pm 2$  °C) that appear driven by ambient temperature. This introduces some variability in the isoprene retention time, but it is accounted for in the analysis of chromatograms (see Section 3.3).”

**P6, line 11. “so that the pre-column is back-flushed”** Is this pre-column heated above trapping temperature during the backflush? It is not clear if the larger molecules are successfully removed during back-flush or if they accumulate.

The pre-column is inside the oven along with the main column, and the oven (hence both columns) is always kept at a higher temperature than the rest of the Pelicase, where the trap is located. As we log the temperature inside the Pelicase at the end of the trapping step, we can look at the difference between oven temperature and trapping temperature. The oven temperature is always 4-8 °C higher than the temperature in the rest of the Pelicase.

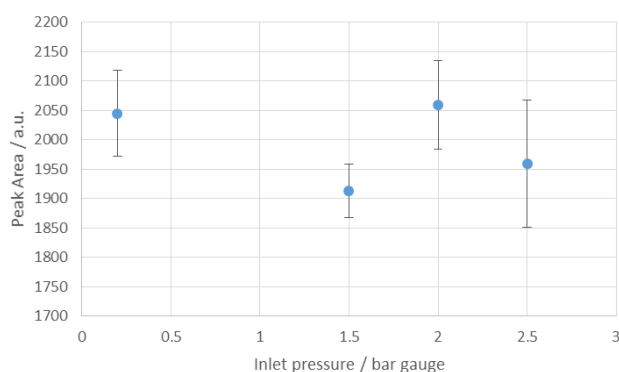
We do not see any signs of carryover between runs, and especially in the blank and calibration runs, so we conclude that larger molecules are successfully removed by the backflush.

**P6, line 30. Figure 3.** Please provide more information (i.e. isoprene mixing ratio, diluent gas, sample humidity) for this example chromatogram.

Figure 3 has been amended include a calibration, a sample and a blank chromatogram with the corresponding fits to the data. The caption has also been amended to include the information requested.

**P7, line 17. The flow through the instrument is driven by either upstream pressure (in the case of the nitrogen and calibration gas flows) or by the pump box (in the case of Samples 1 and 2).** Is the sample pressure measured? From the description here and in Figure 2 (and associated text) it is not clear if the adsorbent trap experiences higher pressure when the cal / blank solenoid valves are actuated, versus when using sample inlets 1 / 2. It is the reviewer’s experience that adsorbent trapping efficiency has a pressure-dependence. Has this been observed by comparison of calibrant gas addition via the cal port versus via a sample port?

Whilst sample pressure is not measured during the instrument routine operation, we have measured the gas pressure upstream of the trap (and downstream of the solenoid valves), and found no difference in pressure between sample, calibration or blank runs. This indicates that the flow restrictors also contribute to regulating the pressure down to ambient. We carried out further experiments in which the same mixture was fed into the instrument at different pressures (1.5-2.5 bar gauge) through valve 3 (calibration port), and also at 0.1 bar gauge through valve 1 (sample 1 port) and found no difference in the resulting integrated peak area, as shown below (error bars indicating 1 standard deviation of at least 10 replicates at each pressure).



**P7, line 40. “controls the altimeter pressure sensor”** Is this the same as the differential pressure sensor described previously (P7, line 21)? And does the Arduino board control this sensor, or just read it?

No, this is a different pressure sensor, and effectively measures ambient pressure. The Arduino board only reads it, and the text has been changed accordingly.

**P8, line 22. “Figure 5 shows a flow diagram”** This figure could be moved to a supplemental materials section to conserve space in the main document.

We feel this figure helps understanding the processing of the chromatogram and wish to retain it in the main text.

**P9, line 2. “next step is to locate the isoprene peak and to fit a Gaussian curve”** It is not clear how this is performed, and could use some more explicit description. Is the user manually locating the peak or is the software algorithm doing this? How is the baseline for the Gaussian curve defined? Is there any evaluation of the goodness of the Gaussian fit to the data? There are instances in data figures throughout the text where negative peak areas or mixing ratios are shown. Is this from a fitted Gaussian with negative peak height?

We have replaced that sentence with the following text to clarify how the peak is located and fitted to:

“From the plot of all calibration chromatograms, the user specifies the regions that are used to fit to the isoprene peak and the baseline. A third-degree polynomial is fitted to the baseline over the user-specified baseline intervals. A Gaussian curve is then fitted to the baseline-subtracted chromatogram over the user-specified peak interval.”

Regarding the evaluation of the goodness of the fit, we retain the RMSE from the fit for each chromatogram (refer to general comment 2 on page 2 for this is used to evaluate sample peaks). The height of the Gaussian is allowed negative values, but this only occurs when isoprene is near or below the detection limit (i.e., blank or night-time runs), or during instrument warm-up. The instances of negative areas (and mixing ratios) mentioned by the reviewer have been reanalysed and amended.

**P9, line 6. “A quadratic curve is fit to this data, which captures any slight deviations from linearity.”** As noted above, the use of a non-linear fit to instrument response should have a physical explanation, especially as both positive and negative coefficients are shown in the text. What is the uncertainty of the second-order coefficient? What amount of additional uncertainty would be added the overall measurement by simply using a linear fit of the calibration data?

This has been amended to a straight line fit. Refer to the answer to the first comment on page 1 for further details.

**P9, line 12. “The Gaussian function has certain boundaries set, to further ensure that it is fitted to the correct peak.”** Please describe exactly which boundaries are set. How is the Gaussian fitting function constrained?

The text now reads:

“Then a Gaussian function, constrained by certain boundaries (e.g., peak width within the average calibration peak width  $\pm 1$  standard deviation, retention time within  $\pm 5\%$  of the interpolated retention time), is fitted to the section of the chromatogram indicated by the interpolated calibration retention times.”

**P9, line 15. “it can be estimated using the column temperatures”** This implies that column temperature is not constant. The temperature variance in ambient sampling should be described (see comment above).

Refer to answer to comment on P6, line 5 (“heated to 40 °C”)

**P10, line 1. “This type of treated cylinder exhibits very good long-term stability for a number of VOCs (Gary Barone et al. Restek Corporation, 2010).”** I don’t understand this reference, and it is not listed in the Reference section.

The Barone citation referred to a patent for the SilcoNert treatment. It has now been replaced by two references (Allen et al., 2018, and Rhoderick et al., 2019) that studied the stability of VOCs in Silconert treated stainless steel cylinders (amongst other types).

**P10, line 2. “The exact isoprene amount fraction in the secondary standard is determined by validating it against the NPL primary standard.”** Can the authors make a statement about the stability of their secondary standards over time? This reviewer has found that secondary isoprene standards made in Aculife [Air Liquide] cylinders can degrade over the timespan of months.

We routinely measure the secondary standards against the NPL primary standard before and after field deployments and we found no statistically significant degradation over the time span of a relatively long field deployment (~ 5 months).

The consensus seems to be to either use Air Products Experis cylinders or SilcoNert2000-treated stainless steel cylinders for the best VOC stability over time (see Allen et al., 2018, and Rhoderick et al., 2019). We have added the following sentence:

“We routinely measure the secondary standards against the primary standard before and after field deployments to account for any degradation over time. However we have found no statistically significant degradation over the time span field deployments (up to 5 months)”.

**P10, line 5. “mixing rations”** should be mixing ratios

Amended.

**P10, lines 10-20. “Calibration frequency is specified by the user . . .”** While the explicit description of the instrument calibration method is welcome, it is probably more appropriate to move this material, along with Figure 6, to a supplemental materials section.

We have edited this paragraph to only include relevant information on the calibration process. We feel figure 6 is useful in illustrating how the calibration areas span the dynamic range of the sample areas and therefore wish to retain it in the main body of the manuscript.

**P10, line 26. “a random mixture of 3, 6, 12, 24 and 48 mL samples”** It appears that the calibration sample volumes used are always significantly smaller than the ambient air sample volumes. Since breakthrough volume is a critical parameter of the sample trap (Section 5.1 of text), I am curious as to why the calibration does not include a sample volume larger than ambient volume.

We typically have standards at higher concentrations than ambient isoprene (5-10 ppb), meaning that a smaller volume of the calibration gas is needed to obtain a peak of area comparable in magnitude to that of a sample run. We agree with the reviewer that avoiding breakthrough is critical, so we are looking to introduce periodic larger calibration volumes in the measurement routine to ensure linearity and check for breakthrough.

**P10, line 30. “The equation for the quadratic fit allows the determination of the fractional isoprene amount in the samples by extrapolation or interpolation”** The use of a quadratic calibration curve with extrapolation seems especially susceptible to the introduction of additional error in reporting mixing ratios.

We have now amended all fits to linear as opposed to quadratic.

**P11, line 1. Figure 6.** The linear fits of the peak areas for the individual calibration volumes versus time do not seem appropriate for this figure, since they are not used in the calibration procedure described in the text (peak area versus calibration sample volume on a weekly time scale) nor discussed in the text. The peak areas of 48mL calibration samples show a significant decay with time that is not apparent in the smaller calibration volumes. Is this statistically significant, and, if so, does this imply breakthrough for large sample volumes?

We have replotted Figure 6 with the linear fits removed. We also realised that the subset of 48 mL peak areas shown in the earlier version exaggerated the negative trend, and have included values at earlier dates. This shows a much less pronounced negative gradient for the 48 mL data, much more in line with that of the other calibration volumes and with the overall trend in the instrument response that we attribute to trap degradation (as shown in Figure 16). Linear fits to the new version of Figure 6 (not shown) indicate that the 48 mL areas decrease by ~6.4% over the timescale shown, comparable to the decrease seen at 12 mL (6.9 %).

Breakthrough would imply some degree of curvature at higher volumes, and we found curvature to be statistically insignificant for all calibration plots.

**P11, line 9. “The x-axis (‘Effective Calibration Concentration’) consists in the calibration volume (in mL) multiplied by the isoprene concentration in the gas standard (in ppb).”**

Isn't this simply calibrant mass or moles, then? Are you attempting to convert these calibration points to equivalent mixing ratio in ambient air? After solving for the ‘Effective Calibration Concentration’ based upon ambient peak area, does the user then divide this ‘Effective Calibration Concentration’ by the sample volume to determine the ambient mixing ratio? The authors should provide the equation for converting peak area and sample volume to mixing ratio.

We have now changed the x-axis for Figure 7 to “number of calibrant moles”. We also added the following text to explain how the ambient mixing ratios are calculated from the measured peak areas:

Using the sample peak area ( $A_{\text{sam}}$ ), the sample volume ( $V_{\text{sam}}$ ) and the intercept ( $c$ ) and gradient ( $m$ ) of the calibration curve, the isoprene mixing ratio in the sample can be calculated using Eq. (2):

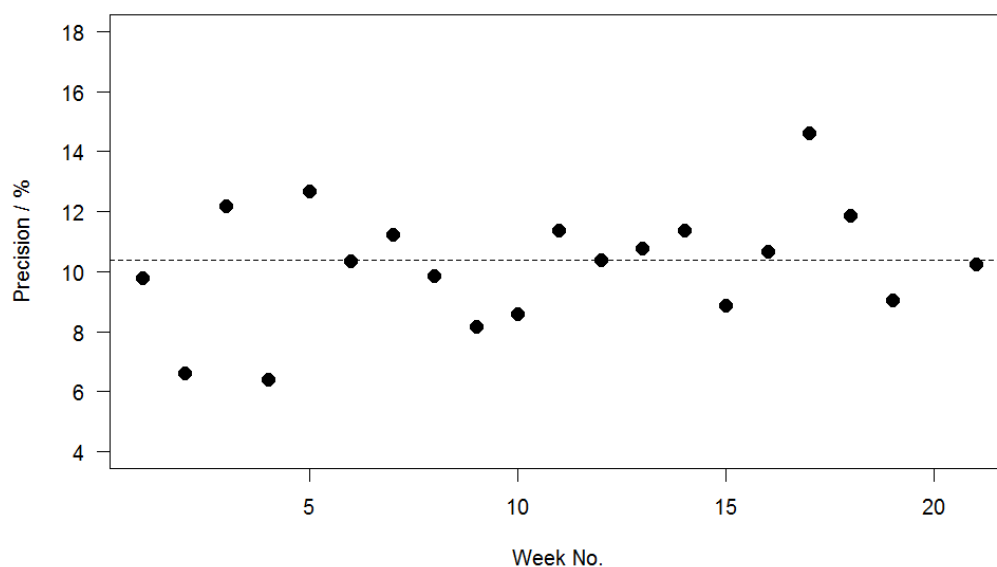
$$X_{\text{sam}} = (A_{\text{sam}} - c)/m \cdot (V_{\text{mol}} / V_{\text{sam}}) \quad (2)$$

**P11, line 15. “The precision of the instrument was determined as the relative standard deviation in isoprene peak area from calibration chromatograms with the same user-specified volume . . .”** In light of the temporal trend in sensitivity discussed later in the text (5.3.2), does this overestimate the precision uncertainty? The authors do not define the length of time that is averaged here, but it appears that the instrument sensitivity decreases on the time-scale of weeks, and therefore we would not expect the peak area here to be a constant.

We have added a sentence at the end of the preceding Section (Section 4.1) to clarify that the data is analysed in weekly segments, so that a calibration curve is obtained for each week of measurements. This is then echoed in Section 4.2, where we add that the precision is also



calculated on a weekly basis. However upon reanalysis of the precision from the WIsDOM campaign, we have revised down the quoted figure (10.4 from 11.3%) as the average precision from the weekly precision estimates, shown in the Figure below.



**P12, line 4.** “The accuracy of the instrument is dictated primarily by the uncertainty in the isoprene amount fraction in the NPL standard, and how this is propagated to the isoprene amount fraction in the secondary gas standard used in the field.” Because the authors have not fully demonstrated that this technique is adequately selective to isoprene, I don’t think this statement is correct. Certainly the uncertainty of the calibrant mixing ratio is a component of accuracy, but perhaps not the primary driver. The intercomparison of two iDirac instruments presented in 5.1 would indicate this as well.

Text amended to say: “One of the main components of the accuracy of the instrument is the uncertainty in the isoprene amount fraction in the NPL standard, and how this is propagated to the isoprene amount fraction in the secondary gas standard used in the field.”

Additional text added to estimate the impact of long-lived co-eluters on the accuracy as per the answer to point 2 on page 2.

**P12, line 9.** “XLGENLINE, a generalised least-squares (GLS) software package for low-degree polynomial fitting (Smith, 2010) is used to estimate the final uncertainty in the isoprene amount fraction in the secondary calibration cylinder by inverse regression from the calibration curve. For most secondary calibration cylinders, this is estimated to ~ 7% at the  $k = 2$  level (providing a coverage probability of approximately 95%). A similar procedure is applied to calibration and sample data from the field to estimate the uncertainty in the ambient isoprene concentrations. This is estimated to ~20-25 % at the  $k = 2$  level.” I found this discussion to be difficult to assess, and reads as simply reporting the output of a statistical software package. Can the authors put this into more explicit terms, e.g. describe what is meant by “inverse regression from the calibration curve”? Also, the comment “most calibration cylinders” is vague – how often do secondary cylinders fall outside this accuracy range? It’s not clear how this technique is extended to the field data; again, please describe the analysis in detail. Finally, it should be noted that the authors here use a  $2\text{-}\sigma$  uncertainty to define accuracy, but a  $1\text{-}\sigma$  uncertainty to define precision above. One uncertainty level should be used for both.

We have rephrased the paragraph to clarify the procedure. For further details we recommend the reference cited in the text. We have also amended the coverage factors from 2 to 1 sigma.

**P12, line 15. Figure 8.** The test cylinder mixing ratio has a negative mixing ratio at the start of the experiment shown. Is this real data, or just an artefact of the analysis? Perhaps the data plot should start after the first standard peak area, at 21:00, 21-Feb-2018.

Those data points are an artefact of the analysis, as the instrument is warming up and we are effectively integrating the baseline. The Figure has been amended.

**P12, line 19.** “. . . the high concentration of isoprene would risk *poisoning the adsorption trap.*” Italic emphasis is mine. Did you intend to use the word “poisoning” here? I interpret that this to mean an irreversible change to the adsorptive strength of the trap, while I believe that you mean that the trap would demonstrate breakthrough due to non-ideal behavior, as described by Peters and Bakkeren (1994).

We have amended the text as follows:

“... a smaller volume should be used to avoid non-ideal behaviour of the adsorbent as described by Peters and Bakkeren (1994)”.

**P12, line 31.** “This is identified as the limit of detection and is calculated for two versions of the iDirac, the grey and the grange instruments.” I found this discussion a bit hard to follow since results from these two instruments were presented without introduction. A sentence or two from the later discussion of these instruments in Section 5.1 would be helpful here. Alternatively, simply cite the LOD for the grey instrument here and discuss the higher LOD observed for the orange instrument in section 5.1.

“grange” changed to “orange”. We have added a reference to Section 5.1 following the introduction of the two instruments.

**P12, line 32.** “This difference is attributed to the traps used (i.e., a trap with more adsorbent would retain more analyte, resulting in a larger signal)” Doesn’t this imply that the traps are not quantitative? If the amount of analyte retained is proportional to the adsorbent mass, this means the traps have a consistent breakthrough, rather than a critical sample volume as described by Peters and Bakkeren (1994). Data provided in the next section (e.g. Figure 11) shows this not to be the case. This explanation does not seem reasonable.

We have amended the text as follows:

“The limit of detection for two versions of the iDirac, the grey and the orange instruments (see Section 5.1 for details), during their deployment in Wytham Woods (See Section 5.2) were 108 ppt and 38.1 ppt respectively. These are higher than the limit of detection determined in the laboratory (46 ppt and 19 ppt respectively). The difference between field and laboratory sensitivity is due to greater noise in the field measurements, as a result of less controlled environmental conditions. The difference in the limit of the detection between the two instruments is attributed to differences in instrumental noise (the noise in the Orange iDirac is 10-20% greater than that from the Grey iDirac), different responses of the PIDs to isoprene, and using traps at different stages of their life cycle (refer to Section 5.3.2 and Figure 16).”

**P13, line 18.** “This under-reading is likely due to differences in the absorbent trap, leading to a lower sensitivity for the orange instrument. This is supported by the calibration curve for the orange iDirac, which curves more at high concentrations, resulting in lower peak height than in the grey iDirac for the same concentration.

**Another artefact of this is that the noise visible on the orange output is greater.”** I am not persuaded by this argument. Why wouldn't calibration account for these differences, irrespective of the curvature of the calibration? Applying a straight-edge to the scatterplot of the two instrument responses shown in Figure 10, I see no significant curvature, i.e. the 6.6% difference appears consistent across the mixing ratio range. See also previous comment for my concern that the adsorbent trap mass is used to explain accuracy differences. The authors may wish to consider alternative explanations, e.g. if the pressures during calibration are the same in both instruments (see comment for P7, line 17). There are two qualitative statements presented here that should be quantified: “curves more at high concentrations” and “noise visible on the orange output is greater.” Finally, it should be noted that the two instruments perform within the specified accuracy for this system (7%), and therefore the performance demonstrated here is acceptable.

Upon closer inspection of the individual chromatograms, we found that the isoprene peaks in the runs from the Orange iDirac exhibited some degree of tailing, particularly evident in the runs where isoprene was higher than 7 ppb. By fitting exponentially modified Gaussians to a subset of these high concentration runs, we found that a normal Gaussians fit underestimated the peak area by approximately 2%. We believe this accounts for some of the observed discrepancy. We have amended the text as follows:

“The results from this experiment are shown in Figure 9. The orange iDirac under-reads by 6.6% relative to the grey iDirac, and this is particularly evident at high concentrations (> 7 ppb). Figure 10 shows this data as a scatter plot of the 15-minute average values from either instrument, again it can be seen that the orange iDirac under-reads slightly. This under-reading is partly attributed to the systematic underestimation of the peak areas from the Orange runs due to peak tailing. Integration of a subset of chromatograms using an exponentially modified Gaussian function showed that a simple Gaussian fit underestimates peak areas from the Orange instrument by up to 2 %. No significant degree of tailing was observed in the runs from the Grey instrument. Despite this slight discrepancy between the output isoprene concentration from the two instruments, the two iDiracs perform within their specified accuracies (see Section 4.2).”

We have also added a statement about peak tailing in the section about accuracy.

We do not believe discussion of the noise in the two instruments is appropriate here, and we have addressed this in the section on sensitivity (Section 4.3; also see answer to the previous comment)

**P14, line 4. Breakthrough tests.** The results presented in this section present a very nice demonstration of the adsorbent trap showing ideal behaviour with a (presumed) single-component isoprene mixture. The citation for this experiment [Peters and Bakkeren, 1994] observed that the breakthrough volume observed in this sort of experiment will be higher than when using a test mixture that includes other compounds, which “may have a pronounced influence on the BTV and thereby on the safe sampling volume of single compounds.” The authors should specify if the test mixture included other species expected in ambient air. If it did not, they should consider how valid the results presented here will be for collection of ambient air.

These tests were carried out using a mixture of 5 ppb isoprene and 5 ppb  $\alpha$ -pinene in a nitrogen balance. We have added this detail to the text.

**P14, line 7. “Each run sampled 10 mL”** Did you mean this? Since you specify varying sample volume in figure 11, I assume this to be a typo and should read “sampled 10 mL min<sup>-1</sup> .”

The text is correct, but the axis label is unclear. It now reads “Cumulative Sample Volume”, indicating this axis is the addition of each individual 10 mL sample run.

**P14, line 8. “isoprene mixture of known concentration”** Perhaps better to say “isoprene mixture at constant concentration.”

Amended to state the actual composition of the mixture (see answer to comment P14, line 4. Breakthrough tests above).

**P14, line 16. Co-elution of interfering species.** I found this section to be a bit trivial, due to the somewhat arbitrary list of species used for this test. I wonder if many of the alkenes used for this work (e.g. 2-methyl-1-pentene) would be expected to be found in ambient air at significant mixing ratios to be of importance as an interferent. The authors note “Work is ongoing to determine the elution time of a wider range of compounds, including oxygenated products from the oxidation of isoprene.” Since the PID is sensitive to many species beyond alkenes (e.g. ketones, aldehydes), I’m not sure if the work here is very conclusive in demonstrating that there would be no interference when measuring ambient air. I would suggest moving this section to a supplemental materials section, or revising with a more exhaustive list of species.

From an analytical perspective alone, the choice of interfering species tested for in this section is not arbitrary at all, as these are the compounds with elution time closest to isoprene. Since the manuscript was first submitted for review, we have tested for acetone and ethanol and found they did not elute in the chromatographic window used. This rules out two common oxygenated VOCs. In addition, the PID is not sensitive to methanol or formaldehyde, thus narrowing down the list of potential interfering species. We have added the following text to the section, which we think makes more relevant to the ambient measurements described in the following pages:

“Similar tests were carried out for acetone and ethanol, and we found they eluted outside of the chromatographic window considered here.”

We have also added a paragraph on the use of peak fit parameters (width, RMSE) to rule out co-elution, in response to point 2 on page 2.

**P15, line 23. “This is an artefact of the trap adsorption process and the resulting tailing of the peak.”** This is a nice explanation of the observed phenomenon. Have the authors considered if the tailing for peaks in ambient air relative to peaks from calibration runs leads to a bias in the peak areas? That is, a Gaussian fit function may miss some of the peak tail for ambient runs relative to calibrations, leading to consistent under-reporting of ambient mixing ratio. This effect could be tested by integrating a subset of peaks to capture all peak area, or by using an exponentially-modified Gaussian fit function.

We have tested a subset of sample chromatograms over a range of concentrations, and found that integrating an exponentially-modified Gaussian as opposed to a simple Gaussian function only leads to an increase in area of ~2%.

**P16, line 11. “Sabah (Malaysian Borneo)”** Could the authors be a bit more specific for this location? Sabah is roughly the same size as Scotland.

Text amended to:

“... the iDirac had its first field deployment at the Bukit Atur Global Atmospheric Watch (GAW) station in the Danum Valley Conservation Area in Sabah (Malaysian Borneo).”

**P17, line 7. “Error! Reference source not found.”** I believe this is a reference to Figure 13.  
[Amended.](#)

**P17, line 15. Figure 14.** For the time series shown, there is a significant time period (16-Nov-2015, 19:00 - 2200) where the mixing ratio trace is significantly below zero. Is this correct or a plotting error? Is this attributable to the “several issues with instrument function”? If the latter, perhaps this time period should be referenced in the text.

[There were actually some issues with baseline shifts in some chromatograms. These should have been vetted at the inspection stage, and have been removed.](#)

**P18, line 12. “5.23.2 Results and discussion”** Should read 5.3.2 Results and discussion.  
[Amended.](#)

**P18, line 17. Figure 15.** There is a drop in the mid-canopy time series on the morning of 7-Nov-2018 that seems anomalous with the other mixing ratio traces and other days shown. The authors may want to confirm that those data pass quality assurance checks.

[There was an error in the data plotted. We have now plotted the correct data.](#)

**P19, line 2. Figure 16.** The calibration curves presented in this figure give me particular concern, as there appear to be consecutive weeks where there is a positive and then negative curvature. Does this seem physically possible? Generally, I found this figure difficult to interpret as I am color-blind and the color scale to distinguish weeks is quite subtle to me. If the underlying data were re-fit with a linear calibration function and a time-series of the slope were presented instead, I suspect that this figure would be much more effective. The x-axis “Effective Calibration Concentration” should have units of mass or moles, as noted for Figure 7.

[The range on the x-axis in the original version of the figure actually exaggerated the curvature of these fits, as the lines were extrapolated well beyond the highest volume \(or “Effective Calibration Concentration”\) on the calibration plot \(typically around 600 “Effective concentration” units, vs the extrapolation to 1000 “Effective concentration” units in the original Figure 16\). As described in the response to the first comment on page 1, we have concluded that the curvature is not statistically significant and have replaced the quadratic fits in Figure 16 with linear fits. We have also added a second panel to the figure with a time series of the gradient of the calibration plot. We have also amended the colour palette to make the figure easier to interpret.](#)

**P19, line 3. “This drift is attributed to the gradual degradation of the trap”** How do the authors separate loss of trapping efficiency from loss of detector sensitivity? If a new sample trap returned sensitivity to the Week 1 level, that would be a useful data point to show.

[We have added an extra point to the plot at week 20, showing the calibration line and its gradient after replacing the trap. This shows an enhanced response, confirming that loss of trapping efficiency \(and not detector drift\) was the cause of the observed drift.](#)

**P19, line 26. “a more sophisticated and interactive control over the oven temperature.”** This statement begs for a presentation of underlying data (oven temperature time trace, retention time drift) to justify this need. Possibly, either could be added to field data time traces in Figure 6, 14 and/or 15 on a secondary axis.

In response to “P6, line 5”, we have added a more in-depth description of the temperature variation and how we deal with its effect on elution times.

**P20, line 9. References.** At least two references (Allen et al., 2018; Helmig et al., 1998) are incomplete. The Barone et al., 2010 reference from the text is missing; see previous comment for P10, line 1.

The Barone reference (a patent) has been replaced with the Allen et al. (2018) reference and an additional reference (Rhoderick et al., 2019), which are the correct works to support that statement. The Allen and Helmig references have been amended.

### References

- Barket et al., J. Geophys. Res., 106: D20, 24301-24313 (2001), doi.org/10.1029/2000JD900562
- Fu, D. et al., Nature Communications, 10: 3811 (2019), doi.org/10.1038/s41467-019-11835-0
- Peters and Bakkeren, Analyst, 119, 71-74 (1994), doi.org/10.1039/AN9941900071

Reviewers' comments are in black, authors' response in blue and changes to the text in red.

## Reviewer #2

This paper thoroughly details the trial of a deployable instrument for remotely measuring isoprene (the main focus of the manuscript) and similar VOCs. There is a great need for calibrated portable instruments that can monitor long term trends out in the field for campaigns and background measurements therefore the iDirac instrument is of great interest, as this can complement reference materials and satellite measurements to give a holistic overview of the atmospheric isoprene distribution. The paper thoroughly introduces the instrumentation and shows the breadth of measurements that have been performed to test it. However, despite the wealth of information specific quantification is often not provided (please see Specific comments). I recommend that this manuscript be accepted once these minor corrections have been addressed.

We thank the reviewer for their feedback and address their comments below.

### General comments

In the introduction it would be useful to explain the importance of isoprene with regards to impact on the OH reservoir in the troposphere, as well as on SOA.

We added the following:

“As a result of its reactivity and the magnitude of its emission rates, determining the global abundance of isoprene is important to understand the oxidising capacity of the atmosphere (Squire et al., 2015) and the formation of SOA, which can affect the optical properties of the atmosphere and in turn impact the climate (Carslaw et al., 2010).”

I think that a bit more detail is required about the instrumentation, particularly with regards to the drier and breakthrough and poisoning of the trap.

Have any tests been performed to assess if the drier removes any VOCs?

Tests were carried out with and without the drier while feeding the instrument the same mixture. No statistically significant differences were observed. We added this sentence to the text:

“Laboratory tests found no statistically significant difference in isoprene peak area between runs using the drier and runs bypassing it.”

How do you recondition the trap, what if terpenes or heavy components stick and reduce trapping ability?

We run blank runs periodically to make sure heavier components are not carried over between runs. However we have not found evidence for carryover. We monitor the trap performance using plots such as the one shown in Fig. 16 and eventually replace it with a new one.

Figure 9

- breakthrough affected by flow rate
- how were the samples pumped into the system
- what happens if you vary the sampling rate?

Upon closer inspection, we now attribute the difference between the two instruments to peak tailing in the chromatograms from the Orange instrument (leading to an underestimate of the peak areas). We have amended this whole section to reflect this.

Similar questions arise from the results depicted in Figure 11.

– breakthrough affected by flow rate

The flow rate is held constant (~ 20 mL/min, the same flow used in the field) so the breakthrough volume obtained here is relevant to our field measurements.

– how were the samples pumped into the system

This is as described in Section 2.2

– what happens if you vary the sampling rate?

We have only investigated this using the sampling flow rate used routinely in the field. An in-depth investigation on the effect of flow rate on breakthrough volume would be valuable, but it is beyond the scope of this work.

It would also be helpful to have a clearer idea of what is meant by the trap becoming “poisoned” is this the result of moisture and what is the impact on uncertainties and sensitivity?

We believe the adsorbent degradation after repeated heat cycles is the principal cause of trap degradation. Typically thermal desorption tubes are replaced after 100 heat cycles. A week of continuous operation of the iDirac in the field consists of ~1000 heat cycles. We have added a second panel to Figure 16 to show the decrease in sensitivity as a function of time.

I strongly suggest that Figure 3 includes information about the isoprene concentration depicted and I would also like error bars added to all figures where required e.g. Figure 7.

Figure 3 has been amended to include a calibration, a sample and a blank chromatogram with peak fits. We also added additional information in the caption regarding the isoprene concentration for each run.

Error bars were added to Figure 7.

Volumes should have an associated uncertainty.

Refer to the answer to comment P10. Line 26.

Finally, I think it would be useful to know why was a Gaussian shape was used for the fitting, have you tried any other peak shapes for fitting e.g. Voigt or speed-dependent Voigt? These might optimise results.

We found that Gaussian curves provided the best fit to the observed chromatographic peaks. We found a marginal improvement with exponentially-modified Gaussians curves.

Specific comments

P1. Line 23. Please change to “Isoprene is an important nonmethane”

We prefer to stress the importance of isoprene relative to other non-methane VOCs, so we have not changed the text.

P1. Line 25. What is the impact of the SOA, please also add references

We added the following:

“As a result of its reactivity and the magnitude of its emission rates, determining the global abundance of isoprene is important to understand the oxidising capacity of the atmosphere



(Squire et al., 2015) and the formation of SOA, which can affect the optical properties of the atmosphere and in turn impact the climate (Carslaw et al., 2010).”

P2. Line 16. Grab samplers: please add example reference e.g. Robinson AD DOI: 10.5194/acp-5-1423-2005  
Reference added.

P2. Line 36. What about trueness?  
“Accuracy” includes trueness and precision according to ISO 5725.

P3. Table 1. Please specify nitrogen purity percentage  
Text amended as follows:  
High Purity Nitrogen (Grade 5.0, or 99.999%)

P4. Figure 1. Does the packaging and foam emit any VOCs?  
Not to our knowledge. However the gas lines are never exposed to the internal packaging during a routine measurement sequence, so chances of VOCs from the foam or packaging affecting the measurement are very low.

P5. Paragraph 2. What is the volume sampled?  
Details on this are given in the “Sample adsorption/desorption system” section further down P5.

P5. Line 30. Why can you not use a non-return valve?  
We have more experience in the use of flow restrictors.

P5. Line 43. Specify the desired volume  
This is specified by the user, and we’ve added the following to this:  
“When the desired volume (as specified by the user in the configuration step – see Section 3) is reached...”

P6. Lines 11-14. Consider combining sentences.  
We believe the paragraph reads better as two shorter sentences.

P6. Line 21. Are there any other VOCs with similar ionisation values or boiling points?  
Most VOCs have ionisation energies in the 8-10 eV range, so they can be detected by the PID (notable exceptions: methanol and formaldehyde). The boiling point is key to determine elution order and potential co-elution, and we have tested for these potential interfering species in Section 5.1.

P6. Figure 3. What concentration does this peak represent? What’s the S/N ratio?  
We have now amended Figure 3 to include a blank, a calibration and a sample peak, with additional information on the gas sampled in the cation. The S/N ratio for the calibration run is 51.8.

P7. Line 7. Should read “in a nitrogen balance”  
Amended.

P7. Line 9. Is the calibration gas purchased or decanted, if the latter please specify how. As stated in the text, these details are given in Section 4.1 and the reader is referred to that Section for further information on the calibration routine.

P7. Line 20. Please specify the reduced pressure  
This is stated on line 23 on the same page (20 kPa below ambient).

P7. Line 23. I think that you mean “nominally” not “typically”?  
Agreed and amended.

P7. Line 38. Is the clock calibrated?  
The clock is not calibrated but we found negligible drift (1-2 seconds) over a 5 months field deployment.

P9. Line 15. What are the criteria for insufficient/sufficient (how many?)

P9. Line 16. What is the criteria for “too great”

In order to capture the fluctuations in elution time brought about by the variations in oven temperature, we recommend having a calibration run at least every six hours. We have amended the text as follows:

“When there are insufficient calibration chromatograms to determine the isoprene peak retention time (e.g., less than 4 calibration runs in a day)...”

P9. Line 26. What is the stability period of the gas standard?

Studies (Rhoderick et al., 2019) have shown that VOC mixtures in Air Products Experis cylinders have a stability of at least 2 years. We have added this to the text.

P10. Line 13. Replace “good practice” with “essential”!  
Amended.

P10. Line 14-19. Please give numbers.

The following text was added:

Typically, a calibration run is performed every 35 sample runs. As the mean duration of a 150 mL sample run is approximately 9 min (consisting of 7.5 min of sampling and 1.5 min of chromatographic run), a calibration run is performed approximately every 5.25 hours.

P10. Line 26. What is the error on the volumes?

We have added the following sentence (and error bars in the relevant plots):

The error in the sampled volumes is dominated by the dead volume in the gas lines before the trap (approximately 1.6 mL), combined with the uncertainty in the measurement of flow rates (1%) and sampling times (0.05%). The overall uncertainty in the volumes is estimated as 50% for 3 mL, 13% for 12 mL, 3% for 48 mL and 1% for 200 mL.

P11. Paragraph 1. Are we talking about intermediate precision or reproducibility?

This is over the timescale of 1 week to 1 month, so strictly speaking it is intermediate precision.

P12. Line 13. What is the lowest volume used – this may impact uncertainty and S/N as the sensitivity is likely to vary with volume size

The volume in the sample runs is held constant throughout a deployment.

P12. Line 31. “the grey and the grange instruments” I think you mean “orange”; please clarify (explain what the difference is before section 5.5).

“Grange” was a typo and has been amended. We have added a reference to Section 5.1 where the two instruments are described more in detail.

P13. Line 11. Specify uncertainty of BOC mixture and add the word “balance” to describe the matrix gas.

Amended.

P13. Line 12. Do you have an offset from losses to the chamber wall?

Potentially, but the point is that both instruments were sampling the same air. So if there were wall losses within the chamber, they would affect both instruments

P13. Line 15. Should be “tee-piece”

Amended.

P13. Line 17. “high” Specify above 8 ppb.

Amended.

P13. Line 22. What happens if you switched the trap? Have you considered the impact of breakthrough at high flow rates?

The rate of gas flows through the trap is roughly constant (20 mL/min  $\pm$ 2%), Switching the traps between the 2 instruments would be an interesting experiment, and would definitely allow to quantify the impact of the traps on the overall instrument performance. However we now attribute the difference between the two instruments to peak tailing in the chromatograms from the Orange instrument (leading to an underestimate of the peak areas). We have amended this whole section of the manuscript to reflect this.

P15. Line 8. Rephrase “pure substance”. Surely there will be impurities in the raw materials? Perhaps state the purity of the reagent?

Rephrased as follows:

“... from the “pure” substance (Sigma Aldrich, purity typically > 98%)...”

P16. Figure 12. What does a blank run look like?

A typical blank run was added to Figure 3.

P17. Line 7. Please resolve “Error! Reference source not found: : :”

Amended.

P17. Line 12. How has this been addressed in subsequent versions?

We implemented an “idle” setting for when the instrument is not used in between measurements. This way, once warmed up, the iDirac can be left on stand-by without requiring another warm-up period when measurement is resumed.

P19. Figure 16. Can you please use a wider colour range?

We have amended the colour palette.

P19. Line 4. Is the poisoning moisture? What impact does this have on the sensitivity and uncertainties attributed?

We believe the adsorbent degradation after repeated heat cycles is the principal cause of trap degradation. Typically thermal desorption tubes are replaced after 100 heat cycles. A week of continuous operation of the iDirac in the field consists of ~1000 heat cycles. We have added a second panel to Figure 16 to show the decrease in sensitivity as a function of time.

P19. Line 20. “can be run autonomously for months” Assuming the trap is not degraded?

Even as the trap degrades progressively, the instrument can run on the same trap for up to 19 weeks as shown in Figure 16. We have added the following sentence to the text:

“provided the performance of the trap is assessed periodically”

# iDirac: a field-portable instrument for long-term autonomous measurements of isoprene and selected VOCs

Conor G. Bolas<sup>1</sup>, Valerio Ferracci<sup>2</sup>, Andrew D. Robinson<sup>3</sup>, Mohamed I. Mead<sup>2</sup>, Mohd Shahrul Mohd Nadzir,<sup>4</sup> John A. Pyle<sup>1,5</sup>, Roderic L. Jones<sup>1</sup> and Neil R.P. Harris<sup>1,2</sup>

5 <sup>1</sup>Department of Chemistry, University of Cambridge, Lensfield Road, Cambridge, CB2 1EW, UK

<sup>2</sup>Centre for Environmental and Agricultural Informatics, Cranfield University, College Road, Cranfield, MK43 0AL, UK

<sup>3</sup>Schlumberger Cambridge Research, Madingley Rd, Cambridge, CB3 0EL, UK

<sup>4</sup>School of Environmental and Natural Resource Sciences, Universiti Kebangsaan Malaysia, 43600, Bangi, Selangor, Malaysia

<sup>5</sup>National Centre for Atmospheric Science, NCAS, UK

10 *Correspondence to:* Neil R.P. Harris (neil.harris@cranfield.ac.uk)

## Abstract

The iDirac is a new instrument to measure selected hydrocarbons in the remote atmosphere. A robust design is central to its specifications, with portability, power efficiency, low gas consumption and autonomy as the other driving factors in the instrument development. The iDirac is a dual-column isothermal oven gas chromatograph with photoionisation detection (GC-  
15 PID). The instrument is designed and built in-house. It features a modular design, with novel use of open-source technology for accurate instrument control. Currently configured to measure biogenic isoprene, the system is suitable for a range of compounds. For isoprene measurements in the field, the instrument precision (relative standard deviation) is  $\pm 14\%$ , with a limit of detection down to  $38 \text{ pmol mol}^{-1}$  (or ppt). The instrument was first tested in the field in 2015 in a ground-based campaign, and has since shown itself suitable for deployment in a variety of environments and platforms. This paper describes  
20 the instrument design, operation and performance based on laboratory tests in a controlled environment, and during deployments in forests in Malaysian Borneo and in Central England.

## 1 Introduction

Isoprene ( $\text{C}_5\text{H}_8$ ) is one of the most important non-methane biogenic volatile organic compounds (BVOC) emitted into the atmosphere. It has a global emission rate estimated at around  $500 \text{ TgC year}^{-1}$  (Guenther et al., 2006) and its oxidation products  
25 make it a major factor determining ozone and secondary organic aerosol production. Emitted by vegetation, it has been linked to temperature regulation, reducing drought-induced stress and other physiological processes within plants (Sharkey, 2013; Sharkey et al., 2008). A dialkene, isoprene is prone to oxidation by reaction with the hydroxyl radical (OH), as well as by ozonolysis and reaction with the nitrate radical ( $\text{NO}_3$ ) (Stone et al., 2011). Isoprene oxidation pathways are complex (Archibald et al., 2010) and result not only in a number of oxygenated volatile organic compounds (OVOCs *e.g.*, formaldehyde,  
30 methacrolein, methyl vinyl ketone) but also in a suite of low-volatility stable products and intermediates that can act as precursors of secondary organic aerosols (Carlton et al., 2009; Claeys, 2004; Liu et al., 2016). As a result of its high reactivity and large emissions, determining the global abundance of isoprene is important to understand the oxidising capacity of the atmosphere (Squire et al., 2015), and the formation of SOA, which can affect the optical properties of the atmosphere and in turn impact the climate (Carslaw et al., 2010).

35 Due to its high reactivity, isoprene is relatively short-lived, with a typical lifetime of the order of one hour in a temperate forest (Helmig et al., 1998) forest. Isoprene emissions are mainly driven by incoming solar radiation and temperature, and as a result exhibit a distinctive diurnal cycle which peaks around midday. Local abundances can change rapidly in response to meteorological variations, such as changes in incoming photosynthetically active radiation (PAR), temperature and  
40 atmospheric dynamics (Langford et al., 2010). High time resolution data is required to capture trends in isoprene concentrations

Formatted: Not Highlight

Formatted: Not Highlight

Formatted: Not Highlight

Formatted: Not Highlight

Formatted: Not Highlight

Formatted: Not Highlight

Formatted: Not Highlight

Formatted: Not Highlight

in real time. It is expected that isoprene emissions will be affected by global change (increasing temperatures, land use change, increasing CO<sub>2</sub>) in the coming decades (Bauwens et al., 2018; Hantson et al., 2017; Squire et al., 2015). However, the overall magnitude and sign of changes in isoprene emissions is still uncertain due to the many variables at play and the uncertainties in our emission models. This, coupled with its large variability, makes it highly desirable to improve the temporal and spatial coverage of isoprene measurements so that our understanding of its emissions via models can be validated against field data.

Measurements of atmospheric hydrocarbons such as isoprene are challenged by the difficulty in making measurements in remote places. To date, in-situ measurements of isoprene have been carried out using existing commercial bench-top instruments, such as gas chromatographs (Jones et al., 2011) and mass spectrometers (Noelscher et al., 2016; Yáñez-Serrano et al., 2015). These techniques differentiate between VOCs either by separation (gas chromatography) or by identification of their molecular ions based on mass-to-charge ratios (mass spectrometry). These instruments, while offering high precision and stability, are not built to withstand field conditions for long periods of time due to their need for power, temperature-controlled environments and speciality carrier gases. This is especially true in under-sampled regions of high isoprene emissions, which are typically in remote or challenging environments (e.g., tropical forests). In these locations instrument size, portability, autonomy, power demand and gas consumption severely limit the length of a deployment. In addition, instrument cost and maintenance limit the number of instruments deployed at any one time, and hence the spatial coverage of a field campaign.

An alternative method to detect environmental VOCs is with grab samples (Robinson et al., 2005). These can either be whole air samples or adsorbent tubes, where air samples (or some specific air components) are collected in an inert vessel and analysed at a later date. While grab samples can be deployed in relatively large numbers, they typically provide low temporal resolution, making this approach unsuitable to capture the rapidly changing concentrations of isoprene. In addition, reactive compounds can degrade over time before analysis, and using this method for long periods, even with some degree of automation, is very time and resource intensive. [Recent work showed that it is possible to retrieve isoprene abundances in the boundary layer using satellite measurements by means of thermal infra-red imaging](#) (Fu et al., 2019). [However, with uncertainties in the range of 10-50%, these retrievals would benefit from further validation from ground-based instrumentation.](#)

All the limitations in the instruments currently used for VOC detection drive the need for a field instrument that is:

- lightweight, so that it is portable and can easily be carried and installed in environments difficult to access with traditional instrumentation;
- low-power, so that it is capable of running off-grid, allowing measurements in locations with no mains power;
- autonomous, so that it minimises operator involvement and maintenance;
- low gas use, so that it minimises the cylinder size required and the number of site visits to replace gas cylinders;
- rugged and durable, so that it can withstand challenging environments; and
- relatively low-cost, so that many instruments can be deployed at one time, maximising spatial coverage.

Here we describe the development and validation of the iDirac, an instrument that fulfils the requirements listed above. It follows on from the philosophy of the  $\mu$ Dirac (Gostlow et al., 2010), with portability, modularity, power efficiency, and autonomy at the centre of its design. The iDirac also incorporates inexpensive microcontroller board processors for advanced control and remote access to the instrument. The core GC instrument and its operation are described in Section 2, while Section 3 presents the software used to control the instrument. Instrument performance is discussed in Section 4, including calibration, accuracy, precision, sensitivity and separation ability. Finally, results from trial runs in the controlled environment of a laboratory and deployments in Malaysian Borneo and Central England are presented in Section 5. Results have been published

on the impact of herbivory on canopy photosynthesis and isoprene emissions in a UK woodland (Visakorpi et al., 2018) and on isoprene concentrations near the Antarctic peninsula (Nadzir et al., 2019).

## 2 Practical description of the iDirac

The iDirac is a portable gas chromatograph equipped with a photoionisation detector (GC-PID): the VOCs in an air sample are separated on chromatographic columns and then sequentially detected by the PID. The instrument is built in-house and is lightweight, low-power and able to operate for up to several weeks or months autonomously. Its specifications are shown in Table 1. Section 2.1 describes the basic outline of the instrument and Section 2.2 describes the specific configuration of the instrument for isoprene.

**Table 1: iDirac specifications**

Power	12 W
Weight	10 kg
Voltage Requirements	10–18 V
Dimensions	22 × 61.6 × 49.3 cm
Carrier Gas	<del>High Purity Nitrogen (Grade 5.0, or 99.999%)</del> <del>High Purity Nitrogen (Grade 5)</del>
Calibration Gas	10 nmol mol <sup>-1</sup> (or ppb) high-accuracy isoprene in nitrogen
Limit of detection	38 pmol mol <sup>-1</sup> (or ppt)
Precision	11 %

### 2.1 Core gas chromatograph physical design

The iDirac is built in a modular fashion, so that the various components are housed in 6 main plastic boxes (Piccolo Polycarbonate Enclosures, IP67) packed in foam inside a protective waterproof case (Peli 1600), as shown in Figure 1. Details on the boxes and their contents are given below, and shown within the instrument in Figure 1:

- Valve Box, containing 8 solenoid valves to control gas flow from the four inlets;
- Control Box, containing microcontroller boards (Arduino and Raspberry Pi), a number of electronic components (e.g. solid state relays), the flowmeter and SD card for data storage;
- Oven Box, containing the dual-column system, (pre- and main columns), heating element and Valco<sup>®</sup> valve;
- PID Box, containing the photoionisation detector (PID);
- Pump Box, containing the pump and pressure differential sensor;
- Power Box, contains power regulators and electrical fuses.

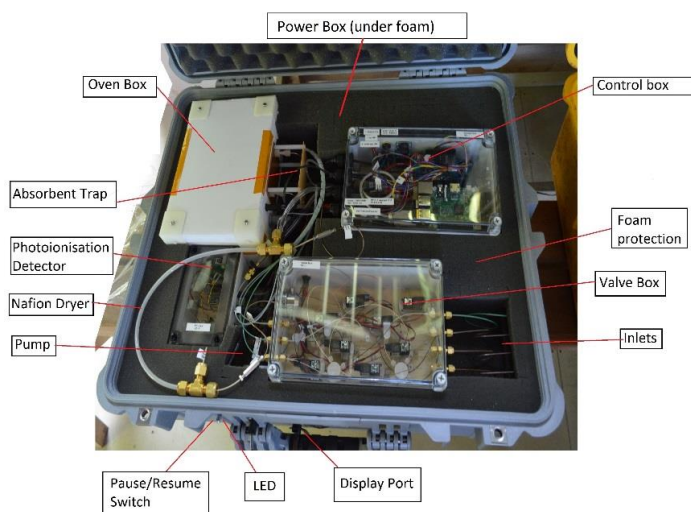


**Figure 1: Interior of the iDirac showing the modular design of its component parts inside the main Peli case (22 × 61.6 × 49.3 cm).**

On the exterior, the iDirac has a power socket, and four inlets for gas input. The inlets are for the nitrogen carrier gas, a calibration gas and two sample lines (Sample 1 and Sample 2) between which the instrument can alternate.

5

The general pneumatic design of the instrument is built around two phases in the analysis cycle which are represented schematically in Figure 2: a loading phase (Load Mode – pink), in which the analyte of interest is pre-concentrated on an adsorbent trap, and an injection phase (Inject Mode - purple), in which the analyte is desorbed from the trap and directed into the oven for separation and, eventually, detection. These two modes are controlled by a 2-way 10-port Valco® valve (VIDV22-3110, mini diaphragm 10 port 2-pos 1/16" 0.75mm, Thames Valco) in the Oven Box, which is activated by pneumatic actuation, by the set of solenoid valves in the Valve Box, and by the pump.

10



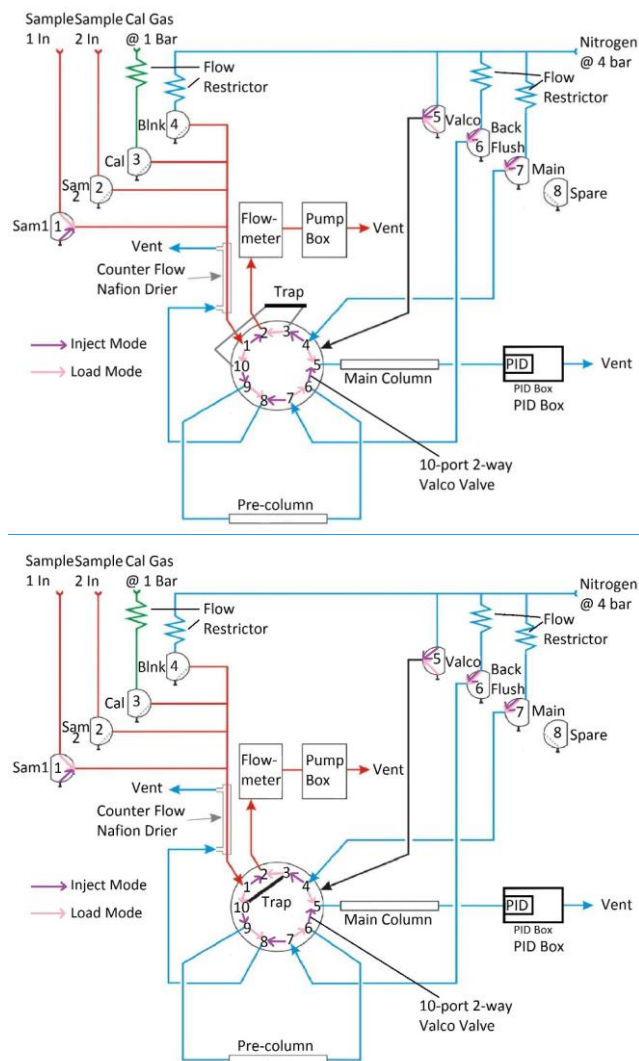


Figure 2: Schematic representation of the iDirac operation. When in Load Mode (valve 5 off - pink), the contents of a gas source chosen between valves 1-4 are pre-concentrated on the adsorbent trap. In Inject Mode (valve 5 on - purple), the VOCs in the trap are injected into the dual-column system for separation and, eventually, detection.

In Load Mode (Valco valve not activated, i.e. valve 5 off), one of four inlet gases (either sample 1, sample 2, calibration gas or blank gas) is selected by switching on the appropriate solenoid valve (valves 1, 2, 3, or 4 respectively). By activating the pump, gas is drawn through the selected inlet valve, dried in a Nafion counter-flow system and passed through an adsorbent trap where the analyte is pre-concentrated. The sampled gas is vented into the Peli® case and then to the outside. A flowmeter is placed in series with the sample flow and measures the gas flow through the trap. Once a pre-defined volume of gas has been sampled, the pump stops and the instrument enters Inject Mode. [Laboratory tests found no statistically significant difference in isoprene peak area between runs using the drier and runs bypassing it.](#)

Formatted: Font color: Auto

In Inject Mode, the trap is flash-heated to ~~approximately~~  $300 \pm 5$  °C for 9 s to desorb the analyte from the adsorbent material. The Valco® valve is then pneumatically activated by switching valve 5 on: the nitrogen carrier is flowed through the trap in the direction opposite to trap-loading, delivering the desorbed compounds into the dual-column system where they undergo chromatographic separation. The oven consists of a pre-column, which screens for large ~~bulky~~ molecules (e.g., the  
5 monoterpenes) whilst allowing smaller molecules through, and a main column, which performs the critical separation of the relevant analytes. The main column eluent is incident on the PID membrane, where the signal from the changing composition of the gas exiting the main column is detected.

More details on the individual parts of this cycle are given below.

**Inlet manifold and sample preparation.** The inlet ports protrude from the side of the Peli® case via 1/16" inch bulkhead unions (Swagelok) and connect directly to the Valve Box, containing 8 solenoid valves that act as gas selectors. The Sample 1 (via valve 1), Sample 2 (via valve 2), calibration gas (via valve 3) and blank nitrogen (via valve 4) lines are all combined in a 4-way Silconert-treated stainless steel Valco manifold (Z4M1, 1/16" manifold 4 inlets, Thames Valco). This manifold leads to the adsorbent trap via a Nafion dryer (Nafion gas dryer 12", polypropylene, PermaPure MD-050-12P-2) which drives excess water vapour out of the gas flow by diffusion through a membrane with a counter flow of dry high-purity nitrogen. Valve 5 is  
15 a direct line from the nitrogen inlet to the Valco valve for actuation, which requires a higher pressure (typically 4 bar). Valves 6 and 7 control the nitrogen flow through the columns: valve 7 activates the nitrogen flow through both columns in Inject Mode (when valve 5 is on), and through the main column only in Load Mode (when valve 5 is off). Valve 6 activates the nitrogen flow through the pre-column for the backflush in Load Mode. The nitrogen counter-flow needed for the Nafion dryer is provided by Valve 6 in Inject Mode and by the pre-column backflush vent in Load Mode. Gas lines downstream from valves  
20 5, 6 and 7 leave the box via manifolds on the side of the box. Valve 8 is a spare valve with no current function.

Flow restrictors upstream from valves 3, 4, 6 and 7 ensure that the flow from the pressurised inlet lines does not exceed the maximum flow through the flowmeter, and also reduce the gas demand of the instrument. The restrictor tubing used for the calibration line is red PEEK flow restrictor (1/32" OD, 0.005" ID) and the one used for the nitrogen lines is black PEEK (1/32" OD, 0.0035" ID). The rest of the tubing is Silconert-treated stainless steel (Thames Restek, 1/16" OD, 0.04" ID), which does  
25 not restrict the gas flow.

**Sample adsorption/desorption system.** From the Nafion drier, the sample gas passes through ports 1 and 10 of the Valco valve and into the adsorbent trap when the instrument is in Load Mode. The trap consists of wide bore stainless-steel tubing (HI-Chrom, 1/16" OD, 0.046" ID) containing one bed of adsorbent material between two beds of glass beads, both crimped in place, with a coiled nichrome wire heating element surrounding the section of the tube corresponding to the adsorbent. [The  
30 nichrome wire has a ceramic electrically insulating coating to prevent shorting with the trap tubing.](#) The adsorption of isoprene and other VOCs takes place on a bed of approximately 10 mg [Graphsphere 2016 \(formerly Carboxen 1016, Supelco, 60/80 mesh, 11021-U\)](#); [Graphsphere 2016 Carboxen 1016](#) is a carbon molecular sieve that has been selected for its optimised recovery rate of unsaturated short chain hydrocarbons upon thermal desorption. Different sorbent materials can be used for other species. The gas exiting the trap, now scrubbed of VOCs, flows via ports 3 and 2 on the Valco valve into the flowmeter (Sensirion, ASF1430) which monitors the flow rate through the trap. This is then integrated across the duration of sampling to calculate  
35 the total volume of gas sampled. When the desired volume ([as specified by the user in the configuration step – see Section 3](#)) is reached, the valves from the sample inlet are closed and the pump is halted to stop the flow of gas through the trap. The heating coil is flash-heated to desorb the analyte from the adsorbent, while the Valco valve is switched to Inject Mode and valve 7 is activated, flushing the desorbed VOCs onto the pre-column in the oven box with the high-purity nitrogen carrier.

**Isothermal oven.** The flow containing the sample leaves the trap and enters the thermally insulated oven box. This enclosure, housed in insulating material (Lightweight display board, Kerbury Group), is heated to 40 °C using a heating element (PTC element enclosure heater, 15W 12-24V 40C) which is fixed to the base-plate of the oven using conductive paste. A fan mixes the air inside the oven to ensure a uniform temperature throughout. [The oven temperature exhibits diurnal variations \(typically](#)

[in the range of  \$\pm 2\$  °C\) that appear driven by ambient temperature. This introduces some variability in the isoprene retention time, but it is accounted for in the analysis of chromatograms \(see Section 3.3\).](#)

The sample is injected onto the pre-column (5% RT-1200, 1.75% Bentone-34, SILPT-W, 100/120, 1.0 mm ID, 1/16"OD SILCO NOC, Custom Packed, Thames Restek, ~70 cm in length) via ports 10 and 9 on the Valco valve. Here, isoprene and other small molecules travel faster through the pre-column than bulky VOCs. After a set time (typically, 30 s), once isoprene has passed through the pre-column, the Valco valve is switched off, with Valve 5 closing and Valve 6 opening, so that the pre-column is back-flushed. This way lighter species, including isoprene, elute onto the main column while larger molecules that are still in the pre-column when valve 5 is switched off are removed from the column system via the back-flush. This is important to avoid large, less volatile species from entering the main column.

The main chromatographic separation occurs on the main column (OPN-RESL-C, 80/100, 1 mm ID, 1/16"OD, SILCO NOC, Custom Packed, Thames Restek, ~70 cm in length), based on the boiling point and polarity of the VOCs. This way, different species elute onto the detector at different times.

**Photoionisation detection system.** The sample is directed from the outlet of the main column into a photoionisation detector (PID). The PID (Alphasense Ltd™, PID-AH) operates by ionising any gas diffusing through a membrane covering a krypton lamp. Near-vacuum UV radiation from the lamp ionises any molecule with an ionisation potential of less than or equal to 10.6 eV. Isoprene, with an ionisation potential of 8.85 eV (Bieri et al., 1977), is readily photolysed and hence detected by the PID with a sensitivity of 140% relative to that of isobutylene, which is used by the manufacturer as a reference compound in terms of PID response. The ions generated by photoionisation produce a voltage change across an electrode system which is converted to a digital signal by an analogue to digital converter (ADC) (16-Bit ADC 4 Channel, Adafruit). The PID is turned on for the duration of the elution from the dual-column system, and the data is collected at a frequency of 5 Hz. The chromatography run finishes once isoprene has eluted from the main column (typically 60-75 s after starting the back-flush). The data from the PID is then saved to a new file on an SD card by the Arduino Mega. A typical chromatogram showing an isoprene peak is shown in Figure 3.

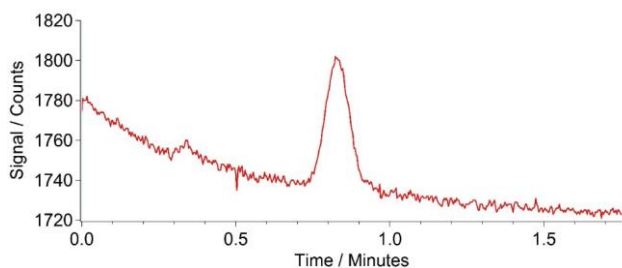
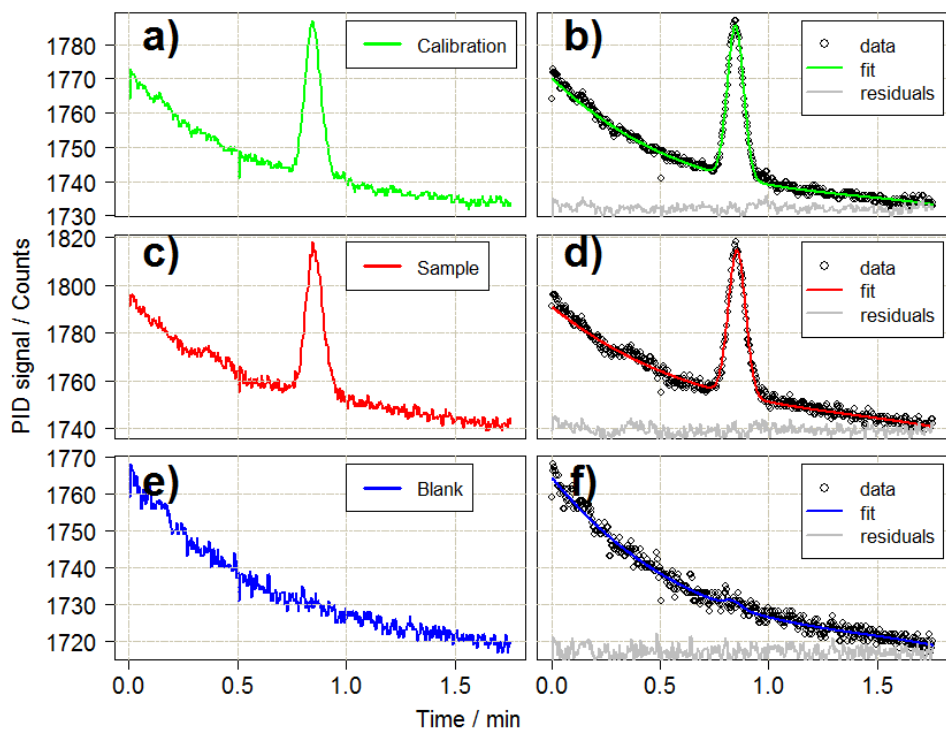


Figure 3: Typical chromatograms for a) calibration, c) sample, and e) blank runs, showing the isoprene peak detected by the PID is around the 0.8 min mark. Panels b), d) and f) show the combined baseline and Gaussian fits to the observed data for each run type. Residuals are offset for clarity. All the chromatograms are from the deployment in Wytham Woods (see Section 5.3). The calibration run is for 12 mL of a 11.6 ppb standard of isoprene in a nitrogen balance. The sample run is for a 150 mL ambient air sample (later quantified as 1.5 ppb isoprene). The blank run is for a 12 mL sample of Grade 5.0 nitrogen.

## 2.2 Instrument operation specifications

- 10 **Carrier gas and calibration gas.** Two gas cylinders are required to operate the iDirac: a pure nitrogen supply and a calibration gas. Nitrogen is used as carrier gas through the dual column system, as sample gas for the blank runs and also to actuate the Valco valve. The nitrogen supply is of at least Grade 5 purity (corresponding to  $\geq 99.999\%$  nitrogen) to minimise interference from impurities with the detection of isoprene. Typically, we use high purity BIP+ Nitrogen (Air Products). The logistics of the measurement dictate the size of the nitrogen cylinder used: for mobile deployments in the field, small portable cylinders
- 15 (1.2 L) are ideal, whilst larger cylinders (10 L) are more suitable for long-term measurement as they minimise the need for

maintenance visits to replace the nitrogen cylinder. Typically, the iDirac can run continuously on a 10 L nitrogen cylinder supplied at 200 bar for approximately 2 months. The calibration gas consists of a binary gas mixture of approximately 10 nmol mol<sup>-1</sup> (or ppb) isoprene in a nitrogen balance stored in a Silconert-treated 500 mL stainless steel cylinder (Sample Cylinder Sulfinert, TPED, 1/4", Thames Restek). The use of cylinders with passivated internal walls minimises the adsorption of isoprene on surfaces, which would introduce biases in the measurement. The accurate concentration of the calibration gas is determined by comparison with a primary gas standard. The calibration routine is described in detail in Section 4.1.

**Power requirements for operation.** The instrument requires a power supply between 9 and 18 V. This can either be mains power, or alternatively, a battery. The incoming power is smoothed and regulated with two regulators to stable 5 V and 12 V outlets. The Arduino board monitors the supplied voltage in between runs in the case of the battery losing charge or power cuts. If the voltage drops, the iDirac switches to a power-save mode, where the oven, PID and valves are turned off to conserve power and the instrument waits for 20 minutes before again checking the input voltage. Once a high enough voltage (typically 9 V) is detected, the various components are turned on again.

**Flow control through the instrument.** The flow through the instrument is driven by either upstream pressure (in the case of the nitrogen and calibration gas flows) or by the pump box (in the case of Samples 1 and 2). The pump box is an air-tight container with an inlet line and a vent. A diaphragm pump (DF-18, Boxer) withdraws air from the pump box and vents it outside, reducing the pressure inside the enclosure. The reduced pressure within the pump box causes air (from the Sample 1 and 2 inlets) to be drawn through the system, via the trap and the flowmeter. A pressure sensor (differential pressure sensor, Phidgets) monitors the pressure differential between the inside and the outside of the pump box. During a pump cycle, the pump is only activated when the pressure differential falls below a pre-specified value (typically nominally, 20 kPa). This method ensures a uniform flowrate and enables control over low flowrates (~ 20 mL min<sup>-1</sup>), thus reducing the uncertainty in the volume integration of the air sampled.

### 3 iDirac software and hardware control and data analysis

The iDirac is controlled using a dual Arduino system: an Arduino Micro board controls the gas flow components of the instrument, whilst the main instrument control is achieved with an Arduino Mega board. These two units communicate with all of the sensors inside the instrument and read their outputs. A Raspberry Pi computer acts as the interface between the user and the Arduino boards. A Python script is run on the Raspberry Pi, allowing the user to configure the instrument with the desired parameters and read the sensor output from that of the Arduino. The Raspberry Pi desktop can be accessed remotely via an ad-hoc network, allowing connection with a variety of interfaces. This control system allows many of the parameters described above (e.g., sample volume, time spent in each column) to be changed.

#### 3.1 Arduino control of internal electronics

The instrument is controlled primarily using an Arduino Mega 2560 board (Arduino Mega 2560, Arduino). This microcontroller has a number of analogue and digital ports and runs Arduino code (C and C++ commands) to control these ports. An SD breakout board is used (microSD Card Breakout Board, Adafruit) to facilitate the use of an SD card to store data in, while a real time clock (RTC) board is used (Real Time Clock, ChronoDot Ultra-Precise, Adafruit) for time-keeping. Figure 4 illustrates the various connections on the Arduino Mega.

An Arduino Micro board (Arduino Micro, Arduino) controls-reads specifically the altimeter pressure sensor (located in the PID box) and the flowmeter, and sends these readings to the Arduino Mega via a serial port. The use of the Arduino Micro is justified as it simplifies the code on the Arduino Mega, particularly as the flowmeter requires the use of a shifter to convert the RS232 serial signal and several subsequent mathematical manipulations. The Arduino boards do not have a shutdown procedure and can simply be unplugged.

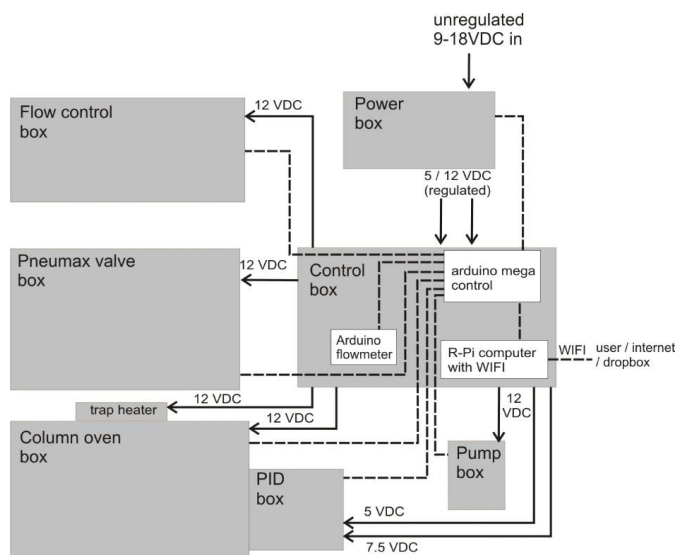


Figure 4: Schematic of Arduino Mega connections

### 3.2 Description of Raspberry Pi user interface

The iDirac uses a Raspberry Pi (Raspberry Pi Model B V1.1, Raspberry Pi) as a user interface, allowing the instrument to be controlled from a familiar desktop environment. The Raspberry Pi uses a Wi-Fi dongle to set up its own ad-hoc network, which can be connected to by laptops and mobile phones in a fashion similar to a standard Wi-Fi network. Once connected to the network, a graphical desktop sharing system such as VNC viewer (VNC Viewer, RealVNC) allows the user to navigate the Raspberry Pi desktop and manipulate the instrument.

Upon opening the Raspberry Pi desktop a purpose-written Python script is launched automatically. A terminal window is opened displaying the serial output from the Arduino Mega and transmitting data to the Arduino Mega via a serial port connection. The latest version of this Python script is freely available (<https://github.com/cgb36/iDirac-scripts>). The Python script decodes incoming serial bytes from the Arduino Mega and displays them in a user friendly command line window. It is also possible to restart and shutdown the instrument from the Raspberry Pi desktop. The Raspberry Pi requires a shutdown procedure, which can be done either physically with a switch on the side of the control box, or from the virtual desktop environment.

### 3.3 Processing of chromatograms

To process numerous chromatograms in an automated fashion, a script was created that uses calibration runs to accurately identify isoprene peaks in the sample runs and convert their integrated peak areas into mixing ratios. This script is written in Mathematica (v11.1.1). Figure 5 shows a flow diagram for the main algorithms of the script. Firstly the data is read in, making sure that all the files are the correct size and do not contain any erroneous runs (e.g., corrupted or truncated files) that may jeopardise the running of the script. Each chromatogram file has an index field, either S, X, C or B which indicate if the chromatogram is a sample 1, sample 2, calibration or blank chromatogram respectively.

The calibration data is processed first. This involves selecting all calibration chromatograms (those with index 'C') and plotting them for visual inspection. From the plot of all calibration chromatograms, the user specifies the regions that are used to fit to the isoprene peak and the baseline. A third-degree polynomial is fitted to the baseline over the user-specified baseline intervals. A Gaussian curve is then fitted to the baseline-subtracted chromatogram over the user-specified peak interval. The next

step is to locate the isoprene peak and to fit a Gaussian curve to it to obtain peak height, width and position (equivalent to elution time) of the fitted Gaussian, as well as the error in the fit (root mean square error, RMSE), are logged. The elution time of the peak is retained in an interpolated function over time. This function is then used to locate the isoprene peak in the sample runs between two calibration runs. The blank runs (with index 'B') are included in this routine as they effectively represent calibrations with zero isoprene concentration. Subsequently, the peak area is plotted against the number of calibrant moles to obtain a response curve. The number of calibrant moles,  $n_{cal}$ , is defined as:

$$n_{cal} = (V_{cal}/V_{mol}) \cdot \chi_{cal} \quad (1)$$

where  $V_{cal}$  is the calibration-sampled volume of the standard during the run,  $V_{mol}$  is the molar volume of an ideal gas, and  $\chi_{cal}$  is the multiplied by the isoprene amount fraction concentration in the gas standard, to obtain a response curve. A straight line is then quadratic curve is fitted to this data, which captures any slight deviations from linearity. Calibration procedures are described in depth in Section 4.1.

The sample chromatograms are then selected as either Sample 1 (runs with index 'S'), or Sample 2 (runs with index 'X') and, as with the calibration runs, they are plotted to visually inspect the data. Following that, we interpolate the retention times from adjacent calibration runs to the time of each sample runs, thus ensuring that the isoprene peak is identified correctly. This effectively takes into account variation in elution time caused by varying oven temperatures, a section of each sample chromatogram is selected as the region where the isoprene peak is likely to reside. This is achieved by interpolating the retention times from adjacent calibration runs to the time of each sample runs, thus ensuring that the isoprene peak is identified

correctly. A baseline is fitted to the sample chromatograms in a similar fashion to those fitted to the calibration ones. Then a Gaussian function, constrained by certain boundaries (e.g., peak width within the average calibration peak width  $\pm 1$  standard deviation, retention time within  $\pm 4$  s of the interpolated retention time), is fitted to this section of the sample chromatogram indicated by the interpolated calibration retention times to calculate all the peak parameters. The Gaussian function has certain boundaries set, to further ensure that it is fitted to the correct peak. Using the sample peak area ( $A_{sam}$ ), the sample volume ( $V_{sam}$ ) and the intercept ( $c$ ) and gradient ( $m$ ) of the calibration curve, the isoprene mixing ratio in the sample,  $\chi_{sam}$ , can be calculated using Eq. (2):

$$\chi_{sam} = (A_{sam} - c)/m \cdot (V_{mol}/V_{sam}) \quad (2)$$

When there are insufficient calibration chromatograms to determine the isoprene peak retention time (e.g., less than 4 calibration runs in a day), it can be estimated using the column temperatures from the nearest calibration runs. If the spacing between calibration points is too great or the calibration is done separately to the sampling, the interpolated calibration retention time values may not span the region where the isoprene peak resides. In this case the column temperature and retention time of the most recent calibration chromatograms are used to define a linear relationship. It is then possible to derive the isoprene retention time from the column temperature of the sample chromatogram.

Formatted: Font: Italic

Formatted: Subscript

Formatted: Font: Italic

Formatted: Subscript

Formatted: Font: Italic

Formatted: Subscript

Formatted: Font: Italic

Formatted: Subscript

Formatted: Font: Italic

Formatted: Subscript

Formatted: Font: Italic

Formatted: Subscript

Formatted: Font: Italic

Formatted: Highlight

Formatted: Not Highlight

Formatted: Highlight

Formatted: Font: Italic

Formatted: Subscript

Formatted: Font: Not Italic

Formatted: Font: Italic

Formatted: Font: Italic

Formatted: Font: Italic

Formatted: Subscript

Formatted: Font: Italic

Formatted: Font: Italic

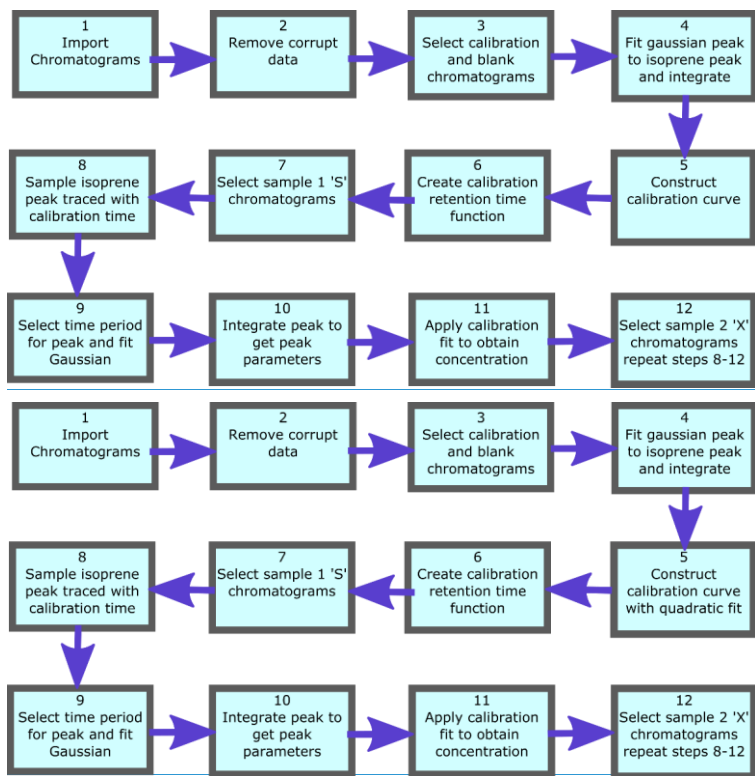


Figure 5: Analysis script flow diagram

#### 4 Instrument performance

##### 5 4.1 Calibration of output chromatograms

The PID response to isoprene is calibrated using a primary gas standard supplied by the National Physical Laboratory (NPL), certified as containing  $5.01 \pm 0.25 \text{ nmol mol}^{-1}$  (or ppb) isoprene in a nitrogen matrix ([uncertainty provided at the  \$k = 2\$  level](#)). The gas mixture is stored in a 10 L -Experis cylinder (Air Products); this type of cylinder has been demonstrated to provide maximum stability ([up to 2 years](#)) for VOC mixtures over time ([Allen et al., 2018](#))(Allen et al., 2018; Rhoderick et al., 2019).

10 The primary standard is only used for calibration in the laboratory; for field deployments, a smaller secondary gas standard is used instead. This is prepared manometrically by diluting a higher concentration parent mixture ( $100 \text{ nmol mol}^{-1}$  isoprene in nitrogen, BOC) to approximately  $10 \text{ nmol mol}^{-1}$  with high-purity nitrogen (BIP+, Air Products). This secondary gas standard is prepared in a 500 mL Silconert-treated stainless steel cylinder (Sample Cylinder Sulfinert, TPED, 1/4", Thames Restek). This type of treated cylinder exhibits very good long-term stability for a number of VOCs ((Allen et al., 2018; Rhoderick et al., 2019)[Gary Barone et al. Restek Corporation, 2010](#)). The exact isoprene amount fraction in the secondary standard is determined by validating it against the NPL primary standard. This way the measurements from the iDirac are traceable to accurate primary standards. [We routinely measure the secondary standards against the primary standard before and after field deployments to account for any degradation over time. However we have found no statistically significant degradation over the time span field deployments \(up to 5 months\).](#)

20 Frequent calibration is needed not only to convert chromatogram peaks into mixing ratios, but also to monitor long-term trends in the detection system, including detector drift and decreasing performance of the adsorbent trap. Any changes in



isoprene elution time, which may be caused by changes in oven temperature, can affect the correct peak assignment in chromatograms with multiple peaks. These effects can be easily addressed if frequent calibration chromatograms (which only have, by definition, one peak) are available.

Calibration frequency is specified by the user in the instrument set-up by selecting the number of samples to run between

5 calibrations. For example, a calibration frequency of '4' would correspond to a run of four sample chromatograms, followed

by a calibration run. ~~No calibrations can be selected by inputting '999' (e.g., when there is no access to calibration gas), whilst~~

~~a calibration only run can be selected by inputting '0'. It is good essential practice to perform a calibration run periodically to~~

10 ~~ensure that the position of the isoprene peak can be traced. Typically, a calibration run is performed every 35 sample runs. As~~

~~the mean duration of a 150 mL sample run is approximately 9 min (consisting of 7.5 min of sampling and 1.5 min of~~

~~chromatographic run), a calibration run is performed approximately every 5.25 hours. The exact number of sample~~

~~chromatograms that can be run in that time depends on the duration of the chromatographic run (which is designated by the~~

~~user by specifying an 'inject time' and a 'backflush time') as well as on the volume of air sampled (also specified by the user),~~

~~which in turn dictates the duration of the step in which the sample is pre-concentrated in the trap.~~

15 The calibration cycle is programmed to be preceded and followed by a blank run, in which the system samples from the high-

purity nitrogen supply from Valve 4. This allows any residual isoprene in the trap to be desorbed before and after calibration,

and to monitor the efficiency of desorption over time.

A calibration curve is obtained by varying the volume sampled in each calibration run. When configuring the instrument, the

user specifies a calibration volume in mL, which is sampled every other calibration run. For the remaining calibration runs,

20 the instrument is programmed to sample a volume picked randomly from 5 possibilities: the user-specified calibration volume,

the user-specified calibration volume multiplied by 2 or 4, and the user-specified calibration volume divided by 2 or 4. For

instance, for a run configured with a calibration volume of 12 mL, half the calibration runs would be of 12 mL samples and

half a random mixture of 3, 6, 12, 24 and 48 mL samples. A typical time sequence of isoprene peak areas from different

calibration volumes is shown in ~~Figure 6~~ ~~Figure 6~~. A calibration curve is then obtained by plotting these peak areas against the

~~number of calibrant moles effective isoprene concentration (as defined in Eq.(1) as the sample volume multiplied by the~~

~~isoprene mixing ratio in the calibration cylinder). The zero concentration moles point is obtained from the blank runs. A~~

~~quadratic straight line is fitted to the calibration data. A typical calibration plot is shown in Figure 7~~ ~~Figure 7~~. The straight line

~~equation for the quadratic fit allows the determination of the fractional isoprene amount in the samples via Eq. (2) by~~

~~extrapolation or interpolation, provided the sample volume and peak area are known. Typically, data is analysed in weekly~~

~~segments, so that a calibration curve is obtained for each week.~~

30 ~~The error in the sampled volumes is dominated by the dead volume in the gas lines before the trap (approximately 1.6 mL),~~

~~combined with the uncertainty in the measurement of flow rates (1%) and sampling times (0.05%). The overall uncertainty in~~

~~the volumes is estimated as 50% for 3 mL, 13% for 12 mL, 3% for 48 mL and 1% for 200 mL.~~

Formatted: Font color: Auto, Not Highlight

Formatted: Font color: Auto

Formatted: Font color: Red

Formatted: Font: Not Bold

Field Code Changed

Formatted: Font: 10 pt, Not Bold

Formatted: Font: 10 pt, Not Bold

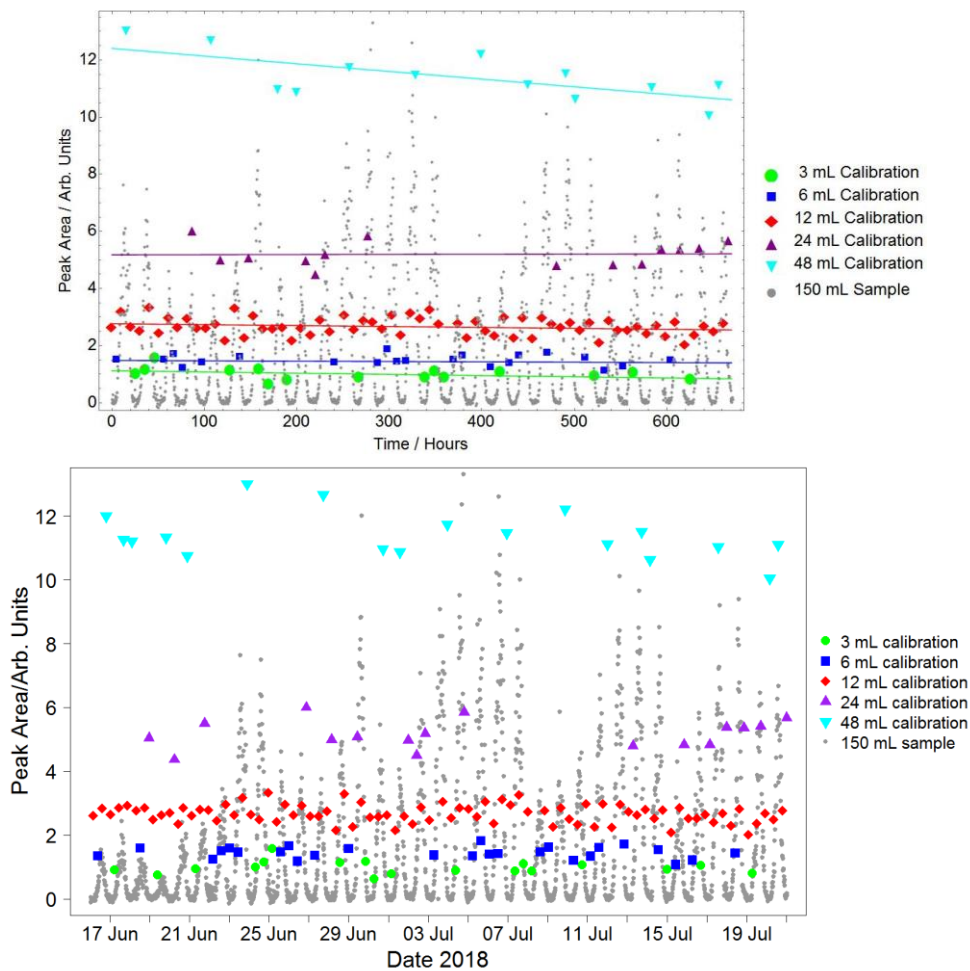
Formatted: Font: 10 pt, Not Bold

Formatted: Font: 10 pt, Not Bold

Formatted: Font: 10 pt, Not Bold

Formatted: Font: Bold

Formatted: Normal, Line spacing: single



5 Figure 6: Typical sequence of isoprene peak areas for runs with varying calibration volumes. These, once split into weekly segments, are used to produce a calibration curve (see Figure 7). The calibration runs with the standard user-specified sampled volume (red data points) are used to calculate the instrument precision on a weekly basis (see Section 4.2). Peak areas from sample runs (grey data points) are also shown to illustrate how the calibration peak areas span the entire range of sample values, minimising the need for extrapolation. This plot was produced using data from the Wytham field campaign (see Section 5.2).

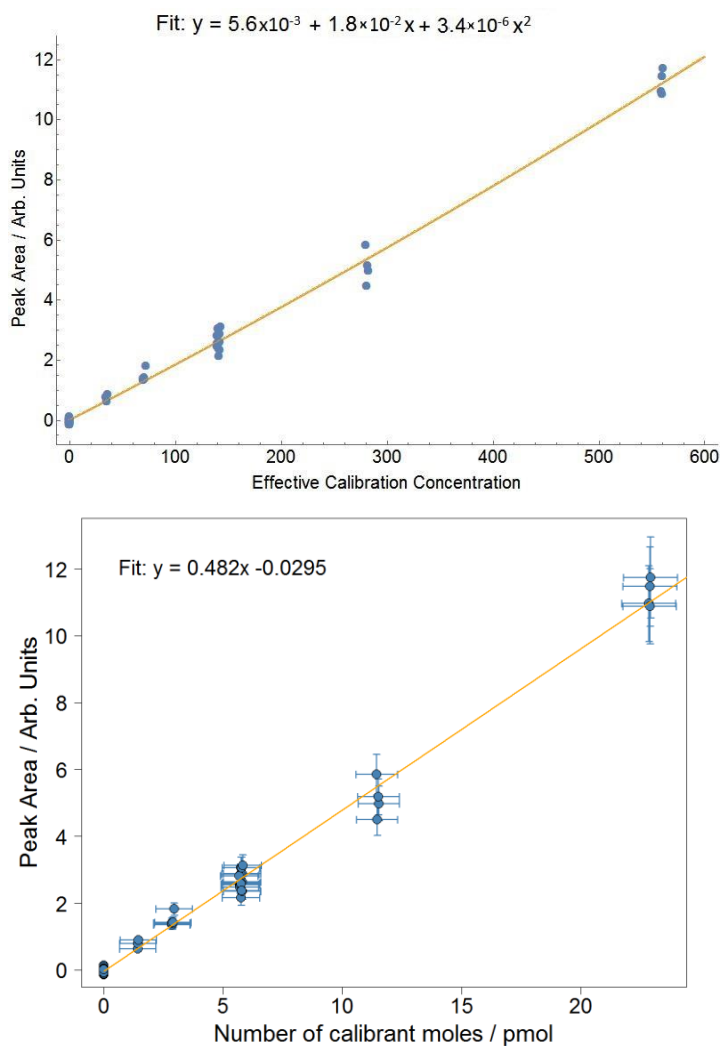


Figure 7: Typical calibration curve plot for isoprene for the week of 02-08/07/2018 from the Wytham field campaign. Error bars in the area correspond to the precision of the measurement ( $\pm 10.4\%$ ). Error bars in the calibrant moles are estimated from the uncertainties in the secondary standard used and in the volume of gas sampled. The x-axis ('Effective Calibration Concentration') consists in the calibration volume (in mL) multiplied by the isoprene concentration in the gas standard (in ppb).

As interpolation carries lower uncertainty than extrapolation, it is important to choose an appropriate value for the user-specified calibration volume, so that the points in the calibration curve span the entire range of the sample runs (as is the case in Figure 6). Typically, 12 mL is suitable in an environment with relatively low ( $< 1$  ppb) isoprene concentrations (e.g. remote oceans), whilst a higher value (20 mL) is more appropriate when measuring in areas such as tropical forests.

#### 4.2 Precision and accuracy of iDirac data

**Precision.** The precision of the instrument was determined as the relative standard deviation in isoprene peak area from calibration chromatograms with the same user-specified volume (typically, more than 50% of the total calibration runs in any given measurement sequence, as detailed in Section 4.1) and from the same calibration cylinder. For instance, in the calibration

sequence shown in [Figure 6](#) and [Figure 7](#), this corresponds to the runs of 12 mL samples. Following analysis of the scatter of these data points, the instrument precision determined is  $\pm 10.34\%$  in the field (compared to  $<5\%$  in the laboratory). This procedure is carried out for each weekly segment of the data means so that the measurement precision can be routinely monitored over time which is especially useful in long deployments.

Formatted: Font: 10 pt, Not Bold

**Accuracy.** One of the main components of the accuracy of the instrument is ~~dictated primarily by~~ the uncertainty in the isoprene amount fraction in the NPL standard, and how this is propagated to the isoprene amount fraction in the secondary gas standard used in the field. It is therefore essential that the concentration of the secondary calibration cylinder is determined as accurately as possible by comparing it to the NPL primary standard. This is carried out in the laboratory, typically before and after each field deployment.

An example of this concentration determination is shown in [Figure 8](#). XLGENLINE, a freely available generalised least-squares (GLS) software package for low-degree polynomial fitting (Smith, 2010) is used to estimate the ~~final~~ uncertainty in the isoprene amount fraction in the secondary calibration cylinder. This is carried out in two steps. First the calibration data (i.e., the peak areas and sampled volumes from the NPL primary standard) is run through XLGENLINE to produce a calibration line with associated uncertainty envelope. In the second step, this calibration curve is used to convert the peak areas from the secondary standard (i.e., the “unknown”) into concentrations and their associated uncertainties by inverse regression from the calibration curve. For most secondary calibration cylinders, this is estimated ~~as~~  $\sim 3.57\%$  (1 standard deviation) at the  $k=2$  level (providing a coverage probability of approximately 95%). A similar procedure is applied to field data calibration and sample data from the field to estimate the uncertainty in the ambient isoprene concentrations (now using the secondary standard for the calibration). This is estimated ~~as~~  $\sim 10-12.5\%$  (1 standard deviation) at the  $k=2$  level.

Co-elution of interfering species can also affect accuracy. Tests targeting specific potential interferents are described in Section 5.1 and show that these species do not overlap with the isoprene peak in the chromatograms. However co-elution with unknown (or not tested for) species, albeit unlikely, can never be fully ruled out. If these species have longer lifetimes than isoprene, the observed night-time abundances attributed to isoprene can be used as the upper limit of potential interference of unknown co-eluters (assuming they are trapped with the same efficiency and have the same PID response as isoprene). The isoprene night-time mixing ratio is 50 ppt for the data shown in both Figures 14 and 15. Therefore we estimate the instrument accuracy for field data as the combination of the propagated uncertainty from the standard (10-12.5 %) and the potential co-elution of long-lived species (50 ppt). This correspond to an overall accuracy of  $\pm 1.2$  ppb for a 10 ppb isoprene sample,  $\pm 0.13$  ppb for a 1 ppb isoprene sample and  $\pm 51$  ppt for a 100 ppt isoprene sample.

Deviations of peak shape from a simple Gaussian function also impact accuracy by introducing a bias in the reported peak areas. However this is limited to high volume, high concentration samples and can add  $\sim 2\%$  to the overall accuracy budget.

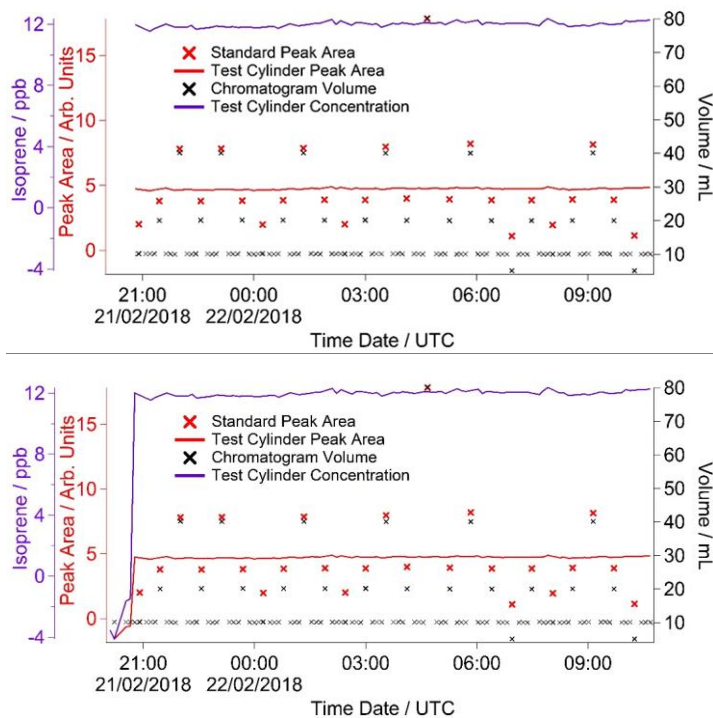


Figure 8: Summary plot of a concentration determination experiment. The primary reference gas mixture is used as the standard in the calibration runs, and the secondary gas mixture under test is used as sample.

#### 5 4.3 Sensitivity of the iDirac to isoprene

The instrument's sensitivity can be adjusted by changing the volume of the sample being analysed. For high concentrations (e.g. strong leaf emissions) a smaller volume should be used ~~as the high concentration of isoprene would risk poisoning the adsorption trap~~ a smaller volume should be used to avoid non-ideal behaviour of the adsorbent as described by (Peters and Bakkeren, 1994). The instrument has an effective upper volume limit of 250 mL (see Section 5.1) and a lower limit of 3 mL.

10 The volume integration becomes unreliable below 3 mL due to the additional uncertainty brought about by the dead volume before the trap (approximately 1.6 mL). On the other hand, when ambient levels of isoprene are low (< 500 ppt), large sample volumes (200 mL) should be used. Sample volumes lower than or equal to 200 mL are used in order not to exceed the trap breakthrough volume (see Section 5.1).

15 The limit of detection is determined for a specific set of runs by allowing a signal-to-noise ratio (S/N) of 3. The blank runs are used to calculate the noise, which is defined as the standard deviation in the PID signal in a section of the blank chromatogram corresponding to the isoprene elution time. The instrument response factor is calculated from the isoprene peak height in the calibration runs and the isoprene amount fraction in the standard. This allows the calculation of the minimum concentration needed to give rise to a signal that would return a S/N of 3. This is identified as the limit of detection and ~~The limit of detection~~

20 ~~can be monitored routinely during fielda deployments and laboratory tests. The limit of detection for is calculated for two versions of the iDirac, the grey and the orange instruments (see Section 5.1 for details), during their deployment in Wytham Woods (See Section 5.2). From the average of 20 calibration chromatograms, the limit of detection of the orange iDirac is were -108 ppt and that of the grey iDirac is 38.1 ppt respectively. These are higher than the limit of detection determined in the laboratory (46 ppt and 19 ppt respectively). The difference between field and laboratory sensitivity is due to greater noise~~

in the field measurements, as a result of less controlled environmental conditions. The difference in the limit of the detection between the two instruments is attributed to differences in instrumental noise (the noise in the Orange iDirac is 10-20% greater than that from the Grey iDirac), different responses of the PIDs to isoprene, and using traps at different stages of their life cycle (refer to Section 5.3.2 and Figure 16). This difference is attributed to the traps used (i.e., a trap with more adsorbent would retain more analyte, resulting in a larger signal), as well as to the performance of the PID detector. The limit of detection can be monitored routinely during a deployment.

## 5 Tests in the laboratory and field deployments

The iDirac has been tested in a series of laboratory evaluations, at a deployment at a field station in a tropical forest in Sabah, Malaysia and in a research forest in Wytham Woods, UK.

### 10 5.1 Laboratory Tests

**Intercomparison of two versions of the iDirac.** Two iDirac instruments (orange and grey) were compared against one another, with the two instruments sampling from a chamber containing a controlled isoprene concentration which was varied over time. The orange and grey iDiracs both had inlets inside the chamber with identical filters (polyethersulfone, 0.45µm pore-size) and the same 1.5 m length of PTFE 1/16" tubing, placed as close to one another as possible. The gas within the chamber was well mixed with two large fans. Gas from a 700 ppb isoprene ( $\pm 5\%$ ) in a nitrogen balance mixture (BOC) was flow-controlled into the chamber at 80 mL min<sup>-1</sup> for different time periods to change the concentration. The chamber was not flushed and the only exchange out of the chamber was slight seepage through several small holes around the inlets. The concentration was varied stepwise from 0 to 12 ppb. The instruments were calibrated using the same calibration standard (8.3  $\pm$  0.6 ppb isoprene in nitrogen), which was connected to both instruments via a tee-piece.

20 The results from this experiment are shown in Figure 9. The orange iDirac under-reads by 6.6% relative to the grey iDirac, and this is particularly evident at high concentrations ( $> 8$  ppb). Figure 10 shows this data as a scatter plot of the 15-minute average values from either instrument, again it can be seen that the orange iDirac under-reads slightly. This under-reading is partly attributed to the systematic underestimation of the peak areas from the Orange runs due to peak tailing. Integration of a subset of chromatograms using an exponentially modified Gaussian function showed that a simple Gaussian fits underestimate peak areas from the Orange instrument by up to 2%. No significant degree of tailing was observed in the runs from the Grey instrument. Despite this slight discrepancy between the output isoprene concentration from the two instruments, it should be noted that the two iDiracs perform within their specified accuracies (see Section 4.2). This under-reading is likely due to differences in the adsorbent trap, leading to a lower sensitivity for the orange instrument. This is supported by the calibration curve for the orange iDirac, which curves more at high concentrations, resulting in lower peak height than in the grey iDirac for the same concentration. Another artefact of this is that the noise visible on the orange output is greater. Adsorbent traps can be replaced on a regular basis to minimise such artefacts.

Formatted: Highlight

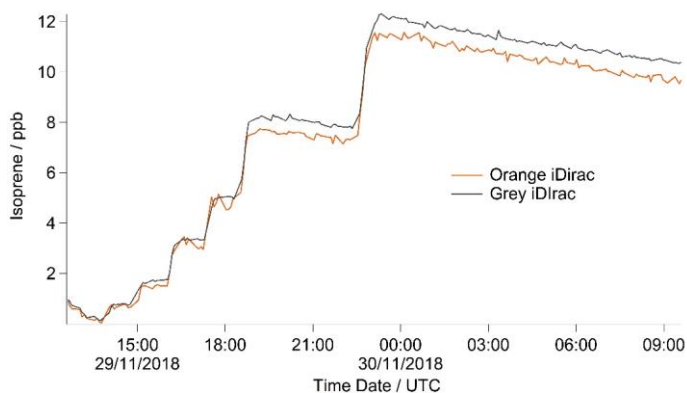


Figure 9: Time series plot showing isoprene mixing ratios from the grey and orange iDiracs

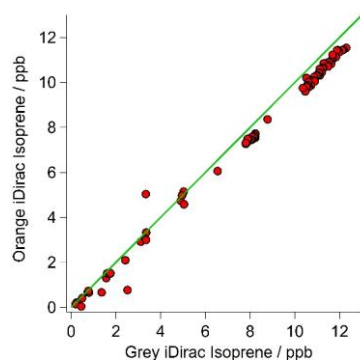


Figure 10: Scatterplot with 1:1 line showing 15 minute average values for the grey and orange iDiracs

5

**Breakthrough tests.** The breakthrough volume for the adsorbent traps used in the iDirac was determined. This is a test which evaluates what volume of gas is so great as to cause isoprene to pass through the trap in a single sample run, and is typically independent of the analyte concentration (Peters and Bakkeren, 1994). This test is performed by placing an additional adsorbent trap in the instrument upstream of the main trap, at the exit of valves 1-4 from the valve box. Each run sampled 10 mL of a mixture of 5 ppb isoprene and 5 ppb  $\alpha$ -pinene in a nitrogen balance isoprene mixture of known concentration. When the breakthrough volume of the additional trap is exceeded, isoprene effectively 'breaks through' from the additional trap onto the main trap, so that it is injected onto the dual column system and a peak is observed in the chromatograms. The sum of all the volumes of the runs in which isoprene was not observed (i.e., pre-breakthrough) gives the breakthrough volume. This value effectively acts as an upper limit of the volume of gas that the instrument can sample. Figure 11 shows a typical example of such test, in which a breakthrough volume of 250 mL was determined. The instrument is therefore set to sample volumes up to 200 mL, so that the breakthrough volume is never exceeded.

10

15

Formatted: Font color: Auto

Formatted: Font: Italic, Font color: Auto

Formatted: Font color: Auto

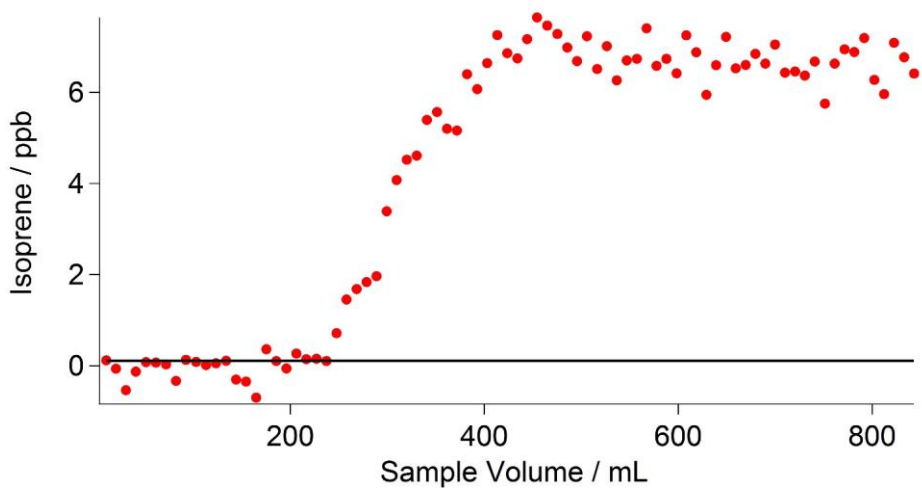
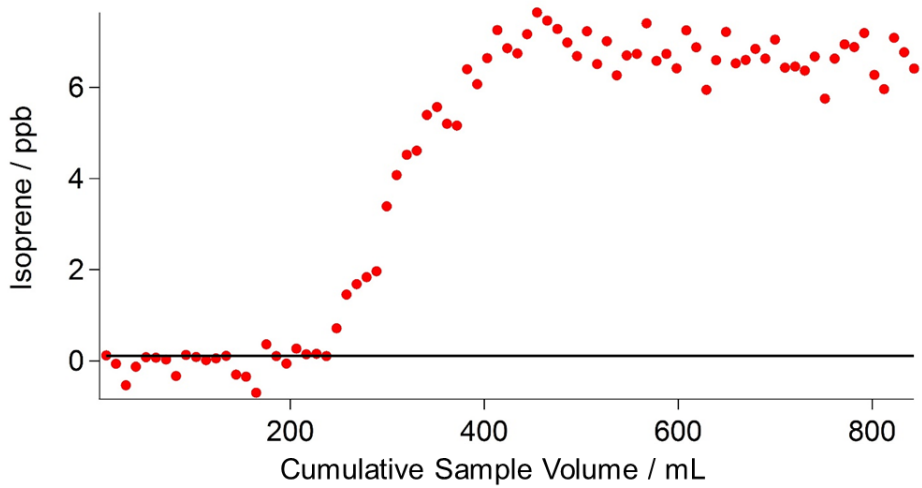


Figure 11: Results of the breakthrough volume tests. Each data point is an individual sample run of 10 mL. A solid black line indicates a threshold (set at LOD of 0.108 ppb), above which the breakthrough volume is exceeded.

5

**Co-elution of interfering species.** The PID used in the iDirac is sensitive to all molecules with ionisation energies less than or equal to 10.6 eV, which includes the vast majority of biogenic and anthropogenic VOCs with the exclusion of ethane, acetylene, propane, methanol, formaldehyde and a number of halogenated hydrocarbons. It is therefore possible that species co-eluting at the same time as isoprene might be detected and erroneously identified as isoprene, thus leading to reporting of spurious concentrations. The stationary phase in the main column is selected to achieve good separation of isoprene from VOCs of similar polarity and boiling point. This is tested in a series of co-elution experiments, in which the elution time of a number of potentially interfering species was determined and their separation from isoprene assessed. The VOCs under test were chosen based on the column specifications reported by the manufacturer, which identified i- and n-pentane, 1-pentene, trans- and cis-2-butene, 2-methyl-1-butene and 2-methyl-1-pentene as potentially co-eluting with isoprene. Gas samples



containing 10-20 ppb of each interfering VOC are prepared in 3 L Tedlar bags by two-step dilutions from the “pure” substance (Sigma Aldrich, purity typically > 98%) using high-purity grade 5.0 nitrogen (purity > 99.999%). For each interfering species, the iDirac alternated between sampling from one of the Tedlar bags and sampling from a gas cylinder containing only isoprene in nitrogen. The results of these measurements are summarised in Figure 12. Figure 12a illustrates overlaid chromatograms for each species, whilst the individual chromatograms are shown in Figure 12b-h. Figure 12i summarises the different elution times taking into account the width of each peak (full-width, half maximum) to better assess separation. The isoprene peak is well separated from all interfering VOCs, while we observe poor separation between cis- and trans-2-butene (which are not separated at all and appear as a single peak in Figure 12d) and 2-methyl-1-butene, as well as between i- and n-pentane. [Similar tests were carried out for acetone and ethanol, and we found they eluted outside of the chromatographic window considered here.](#) These results lend confidence to the unequivocal assignment of the isoprene peak in each chromatogram. Work is ongoing to determine the elution time of a wider range of compounds, including oxygenated products from the oxidation of isoprene.

Co-elution and multiple peaks appearing in a chromatogram are also addressed in the Mathematica script described in Section 3.3. To ensure that the isoprene peak is correctly assigned, the script looks for a peak in a relatively narrow region of the chromatogram, which is based on an interpolation of the elution time from the two nearest calibration runs. This algorithm has relatively low tolerance, so that peaks that are more than 4 s away from the predicted isoprene elution time are not considered. We observe a consistent discrepancy in isoprene elution time between the calibration and sample runs. The elution time of isoprene is typically 1.7 s greater in a sample run than in a calibration run. This is an artefact of the trap adsorption process and the resulting tailing of the peak. For large volumes and low concentrations (e.g., a 150 mL field sample at 0.5 ppb), the isoprene band in the adsorbent trap is very broad and resides in the trap for a longer time, so it tails very strongly. For a high-concentration low-volume sample (e.g., a 12 mL calibration run at 10 ppb), the isoprene band in the trap adsorbent is very sharp; it desorbs quickly and hence it tails less. This difference in elution times is much smaller than the distance to nearest interfering species (2-methyl-1-pentene, which elutes ~7 s before isoprene).

Formatted: Font color: Auto

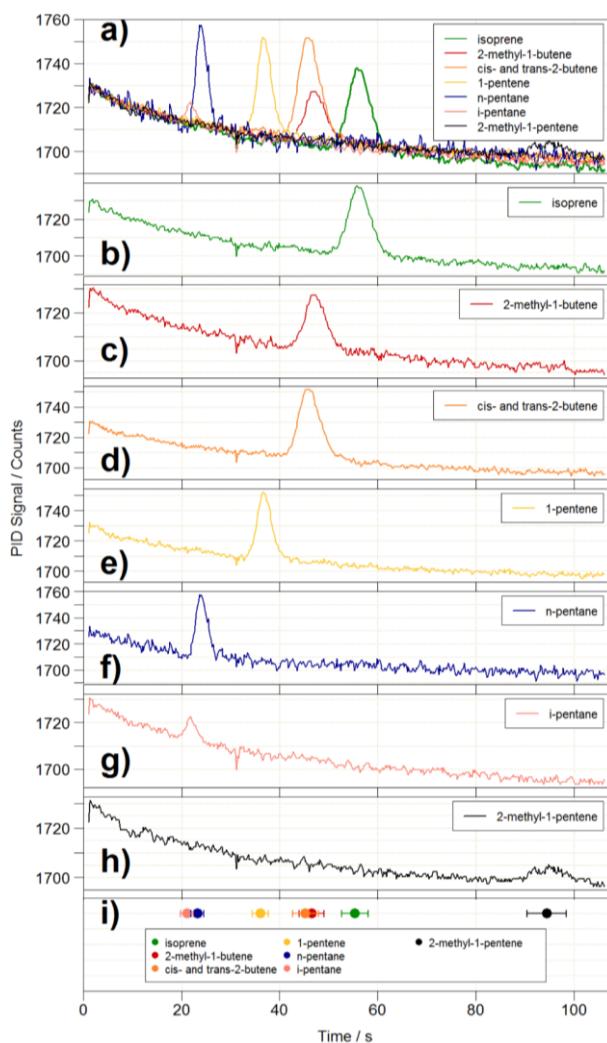


Figure 12: Results of the co-elution tests on the iDirac. a) Overlaid chromatograms of isoprene (green line) and six potential interfering species: 2-methyl-1-butene (red line), cis- and trans-2-butene (orange line), 1-pentene (yellow line), n-pentane (blue line), i-pentane (pink line) and 2-methyl-1-pentene (black line). The chromatograms of each individual species are shown in panels b)-h). The co-elution tests are summarised in h), where the elution time of each species (filled circles) is plotted along with its peak width (FWHM, error bars) to assess peak separation.

Peak width and RMSE from the Gaussian fit, retrieved from the fitting routine described in Section 3.3, can also be used to evaluate the presence of co-eluting species. An additional peak overlapping to some degree with the target isoprene peak in a sample run would cause a change in the peak shape. This would result in values for the fitted peak width and RMSE that are different from those from the calibration runs. For this reason, we use the width and RMSE from the calibration runs to define a range of acceptable peak widths and RMSE (equal to the mean value  $\pm 1$  standard deviation). Any peaks from sample runs exceeding this range are flagged up for further analysis.

**Long-Term Tests.** The performance of the instrument in the field for long periods of time has been assessed in several deployments. These are described in detail in Section 5.2

Formatted: Normal

## 5.2 Deployment of the iDirac in Sabah, 2015

Following laboratory development and testing, the iDirac had its first field deployment [in-at the Bukit Atur Global Atmospheric Watch \(GAW\) station in the Danum Valley Conservation Area in Sabah, Sabah](#) (Malaysian Borneo) as part of the Biodiversity and Land-use Impacts on Tropical Ecosystem Function (BALI) Plant Traits campaign. This campaign ran from May to December 2015. The instrument was principally used to carry out individual leaf measurements in the field. The results from the individual leaf measurements are being written up for publication elsewhere.

The other type of measurements taken in Sabah during this timeframe were longer duration runs, in which the instrument took autonomous measurements of ambient air at the field site continuously. These measurements consisted in attaching the iDirac to a tree at a height of approximately 1 m, with a battery and a 1.2 L N<sub>2</sub> cylinder attached to it, and running repeat samples until either the battery ran flat or the gas supply was exhausted. The aim of these measurements was to obtain an isoprene diurnal profile and observe how this varied with different types of forest. These tests also allowed us to test the feasibility of leaving the instrument running for long periods of time. A picture of the iDirac measuring ambient air in the rainforest in Borneo is shown in [Figure 13](#).

The ambient air measurements demonstrated that the instrument can easily measure the changes in isoprene concentration in the ambient air and that the inlet drying system could cope with the high humidity of the rainforest. An example from a secondary forest site is shown in Figure 14. This was the first deployment for the iDirac, and it proved to be a success in taking reliable measurements. It also highlighted areas for instrument development (e.g., calibration routine) and several issues with instrument function (e.g., warm-up time) that had been addressed in subsequent versions.



Figure 13: iDirac deployed in a tropical forest environment

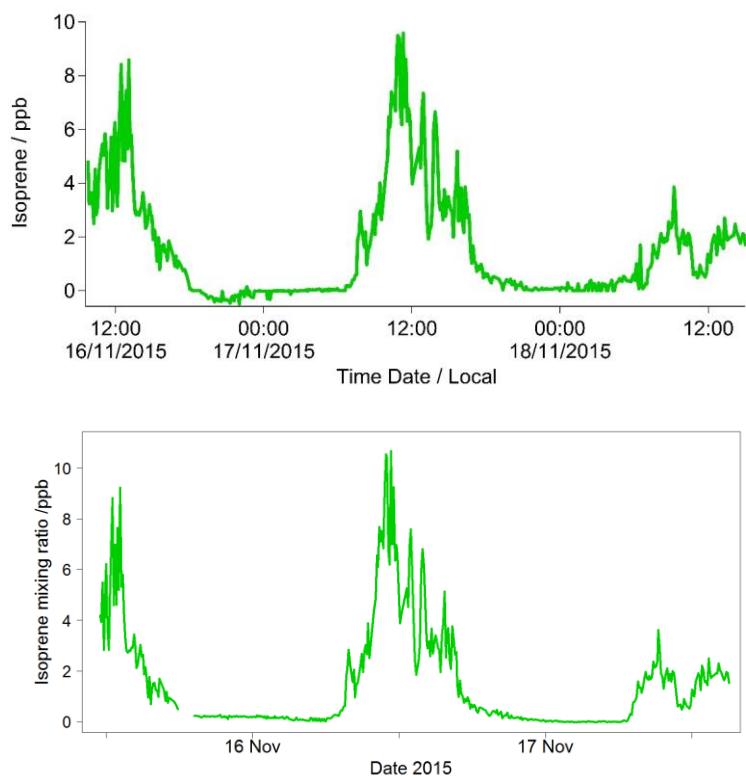


Figure 14: Time series for isoprene at secondary forest site in Sabah (Malaysian Borneo) in 2015

### 5.3 Deployment of the iDirac in Wytham Woods (University of Oxford)

#### 5 5.3.1 Experiment description

The instrument was deployed at Wytham Woods (Oxfordshire, UK), a temperate mixed deciduous forest owned and managed by the University of Oxford. A large fraction of trees at this site are Pedunculate Oaks (*Quercus robur*), which are known strong isoprene emitters (Lehning et al., 1999). One iDirac was deployed on the canopy walkway facility, a platform ~15 m above ground resting on a scaffolding support allowing access to crown-level measurements, while another iDirac was installed at ground level. As each instruments has two inlets, this allowed sampling at four heights across the canopy with a view to investigate the isoprene concentration gradient within the canopy. Both iDiracs were run off-grid, powered only by solar-powered batteries. The experiment and results are described in detail [inby Ferracci et al., n.d.](#), [Ferracci, et al.\(2020\), in prep](#) and [Otu-Larbi et al.; \(2019\)](#). Data was collected from May – October 2018, and here the performance of the instruments is assessed for more than five months of continuous use in a forest environment.

#### 15 5.3.2 Results and discussion

The iDirac captured isoprene concentrations from 25 May to 29 October 2018. Gaps in the data were generally due to power issues arising from insufficient solar charging of the batteries. A section of the isoprene time series is shown in Figure 15. The diurnal pattern of isoprene is clearly visible, and the vertical concentration gradient is also apparent.

Formatted: Italian (Italy)

Formatted: Italian (Italy)

Formatted: Font: Italic, Italian (Italy)

Formatted: Italian (Italy)

Field Code Changed

Field Code Changed

Formatted: Italian (Italy)

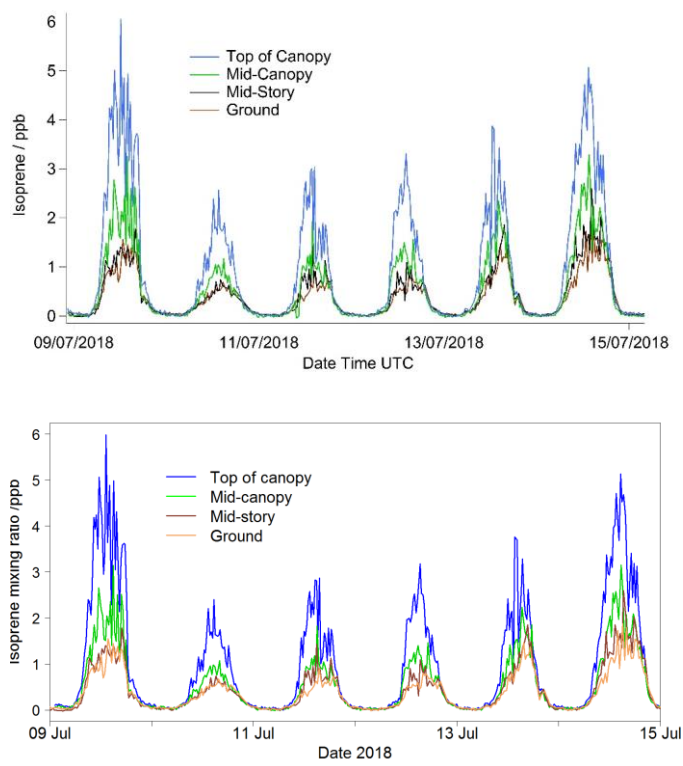


**Figure 15: Portion of the isoprene mixing ratio time series measured at Wytham Woods (UK) at four heights within a forest canopy in the summer of 2018.**

- 5 The iDirac proved capable of measuring isoprene abundances continuously through the day, spanning from concentrations as high as 8 ppb in the height of the summer and to effectively zero at night-time.
- The lifetime of the absorbent trap can be assessed by examining the calibration curves over time. The dataset is analysed in weekly segments, with a calibration curve constructed for each week. This allows for the calibrated data to account for any drift in sensitivity. The calibration plots exhibit a clear drift as time progresses, as shown in Figure 16, with calibration chromatograms later in the time series showing lower peak area for the same concentration. [Once the trap is replaced, higher sensitivity is recovered \(shown as the green dashed line in Figure 16a and the green square in Figure 16b\).](#)
- 10

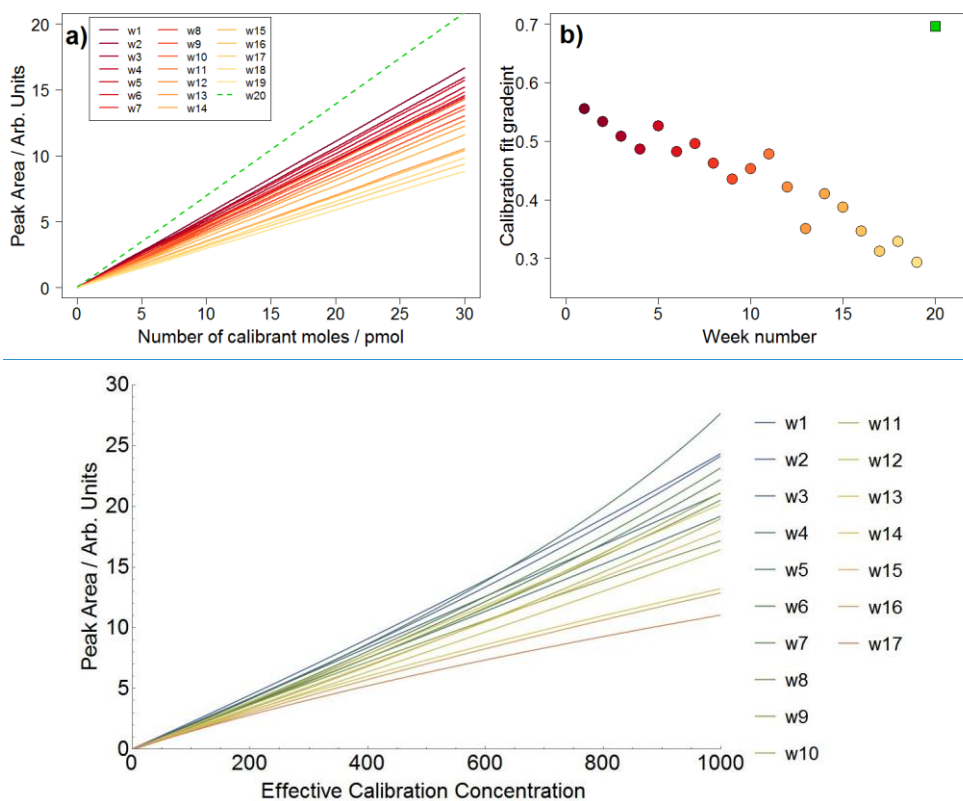


Figure 16: a) Calibration curves plotted in weekly intervals, showing decreasing sensitivity over time (solid lines). The green dashed line is the calibration plot obtained once the trap was replaced. b) Time series of the gradients of the calibration plots showing decreasing sensitivity (filled circles). The green square represents the calibration plot gradient obtained after replacing the trap.

This drift is attributed to the gradual degradation of the trap as a result of repeated absorption/desorption cycles, with exposure to high concentrations of VOCs and oxygen. As each week of data represents approximately 1000 absorption/desorption cycles, it is likely that the adsorbent in the trap becomes 'poisoned' or degraded over time and eventually needs to be replaced.

We are contemplating ways to mitigate this effect, including using a combination of adsorbent materials within the trap so that large VOCs can be prevented from poisoning the adsorbent bed sensitive to isoprene.

A slight curvature can be seen in the calibration curves. This behaviour increases over time and is attributed to the occurrence of a slight breakthrough, as at high concentrations and/or high volumes, some isoprene is not absorbed by the trap. This further supports the implementation of frequent calibration runs in the current measurement sequence used.

Decreasing sensitivity would obviously affect the limit of detection of the instrument. During a particularly long deployment such as that in Wytham Woods, it is important to monitor the sensitivity by means of plots such as that in Figure 16 to establish better when the trap needs to be replaced.

## 6 Conclusions and future work

We described the development and subsequent deployment of the iDirac, a novel autonomous GC-PID for isoprene measurements in remote locations. The instrument pre-concentrates ambient VOCs on an adsorbent trap and then separates

them in a dual column system kept in an isothermal oven before detection by a photoionisation detector, achieving a limit of detection for isoprene down to 38 ppt. The rugged design and modular construction make the instrument easily customisable, while the open source software control results in a straightforward instrument configuration. Designed for field deployments in remote environments with limited power supply, the iDirac weights 10 kg (excluding gas supply), consumes minimum power and gas, can be run autonomously for months with little maintenance ([provided the performance of the trap is assessed periodically](#)) and can be exposed to harsh environmental conditions. The sensitivity and linearity of the instrument response can be tracked effectively with regular calibrations, increasing confidence in the quality of the data. The instrument has been demonstrated to function as desired in a tropical and temperate forest in two lengthy field campaigns, in particular in summer 2018 in an Oxfordshire forest with near continuous operation for almost 6 months. While this paper focused on using the iDirac for isoprene measurements, the instrument configuration can be changed to target different analytes. Future work will focus on monitoring different VOCs (e.g., DMS and ethylene), as well as improving on some of the current limitations of the instrument, such as implementing a more sophisticated and interactive control over the oven temperature. [An intercomparison in real ambient air with more established VOC monitoring instrumentation \(such as that described by \(Barket et al., \(2001\)\) will also help to better evaluate the accuracy of the iDirac.](#)

Formatted: Font color: Auto

#### Acknowledgements

C. Bolas acknowledges and thanks the Natural Environmental Research Council (NERC) for the Doctoral Training Partnership studentship. The research was carried out and supported with funding from the BALI project (NE/ K016377/1) . In the field we would like to thank S. Both of the University of New England, U. Kritzler of the University of Manchester, and the teams at BALI and SAFE for their support. For additional support in Borneo, many thanks to the Malaysian Meteorological Department and Universiti Malaysia Sabah. In addition, we thank Y. Malhi of the University of Oxford for help in deploying at Wytham Woods research forest. For his technical expertise and help, we gratefully acknowledge R. Freshwater at the University of Cambridge.

#### References

- Allen, N. D. C., Worton, D. R., Brewer, P. J., Pascale, C. and Niederhauser, B.: The importance of cylinder passivation for preparation and long-term stability of multicomponent monoterpene primary reference materials, *Atmos. Meas. Tech.*, 11(12), 6429–6438, doi:10.5194/amt-11-6429-2018, 2018.
- Archibald, A. T., Jenkin, M. E. and Shallcross, D. E.: An isoprene mechanism intercomparison, *Atmos. Environ.*, 44(40), 5356–5364, doi:10.1016/j.atmosenv.2009.09.016, 2010.
- Barket, J., Julia, J., Hurst, M., Couch, T. L., Shepson, B., Riemer, D., Hills, A. J., Apel, E. C., Hafer, R., Lamb, K., Westberg, H. H., Farmer, T., Stabenau, E. R. and Zika, R. G.: Intercomparison of automated methodologies for determination of ambient isoprene during the PROPHET 1998 summer campaigns, *J. Geophys. Res.*, 106, 2001.
- Bauwens, M., Stavrakou, T., Müller, J., Schaeybroeck, B. Van, Cruz, L. De, Troch, R. De, Giot, O., Hamdi, R., Termonia, P., Laffineur, Q., Amelynck, C., Schoon, N., Heinesch, B., Holst, T., Arneth, A., Ceulemans, R., Sanchez-lorenzo, A. and Guenther, A.: Recent past ( 1979 – 2014 ) and future ( 2070 – 2099 ) isoprene fluxes over Europe simulated with the MEGAN – MOHYCAN model, , 3673–3690, 2018.
- Bieri, G., Burger, F., Heilbronner, E. and Maier, J. P.: Valence Ionization Energies of Hydrocarbons, *Helv. Chim. Acta*, 60(7), 2213–2233, doi:10.1002/hlca.19770600714, 1977.

- Carlton, A. G., Wiedinmyer, C. and Kroll, J. H.: A review of Secondary organic aerosol (SOA) formation from isoprene, *Atmos. Chem. Phys.*, 9(14), 4987–5005, doi:10.5194/acp-9-4987-2009, 2009.
- Carlsaw, K. S., Boucher, O., Spracklen, D. V., Mann, G. W., L. Rae, J. G., Woodward, S. and Kulmala, M.: A review of natural aerosol interactions and feedbacks within the Earth system, *Atmos. Chem. Phys.*, 10(4), 1701–1737, doi:10.5194/acp-10-1701-2010, 2010.
- Claeys, M.: Formation of Secondary Organic Aerosols Through Photooxidation of Isoprene, *Science* (80-. ), 303(5661), 1173–1176, doi:10.1126/science.1092805, 2004.
- Ferracci, V., Bolas, C. G., Freshwater, R. A., Staniaszek, Z., Jaars, K., Otu-Larbi, F., King, T., Beale, J., Malhi, Y., Waine, T. W., Jones, R. L., Ashworth, K. and Harris, N. R. P.: Continuous isoprene measurements in a UK temperate forest for a whole growing season: effects of drought stress during the 2018 heatwave, *Geophys. Res. Lett.*, submitted, n.d.
- Fu, D., Millet, D. B., Wells, K. C., Payne, V. H., Yu, S., Guenther, A. and Eldering, A.: Direct retrieval of isoprene from satellite-based infrared measurements, *Nat. Commun.*, 10(1), doi:10.1038/s41467-019-11835-0, 2019.
- Gostlow, B., Robinson, A. D., Harris, N. R. P., O'Brien, L. M., Oram, D. E., Mills, G. P., Newton, H. M., Yong, S. E. and Pyle, J. A.:  $\mu$ dirac: An autonomous instrument for halocarbon measurements, *Atmos. Meas. Tech.*, 3(2), 507–521, doi:10.5194/amt-3-507-2010, 2010.
- Guenther, A., Karl, T., Harley, P., Wiedinmyer, C., Palmer, P. I. and Geron, C.: Estimates of global terrestrial isoprene emissions using MEGAN (Model of Emissions of Gases and Aerosols from Nature), *Atmos. Chem. Phys.*, 6(11), 3181–3210, doi:10.5194/acpd-6-3181-2006, 2006.
- Hantson, S., Knorr, W., Schurgers, G., Pugh, T. A. M. and Arneth, A.: Global isoprene and monoterpene emissions under changing climate, vegetation, CO<sub>2</sub> and land use, *Atmos. Environ.*, 155, 35–45, doi:10.1016/j.atmosenv.2017.02.010, 2017.
- Helmig, D., Greenberg, J., Guenther, A., Zimmerman, P. and Geron, C.: Volatile organic compounds and isoprene oxidation products at a temperate deciduous forest site, *J. Geophys. Res. Atmos.*, 103(D17), 22397–22414, doi:10.1029/98JD00969, 1998.
- Jones, C. E., Hopkins, J. R. and Lewis, A. C.: In situ measurements of isoprene and monoterpenes within a south-east Asian tropical rainforest, *Atmos. Chem. Phys.*, 11(14), 6971–6984, doi:10.5194/acp-11-6971-2011, 2011.
- Langford, B., Misztal, P. K., Nemitz, E., Davison, B., Helfter, C., Pugh, T. A. M., MacKenzie, A. R., Lim, S. F. and Hewitt, C. N.: Fluxes and concentrations of volatile organic compounds from a South-East Asian tropical rainforest, *Atmos. Chem. Phys.*, 10(17), 8391–8412, doi:10.5194/acp-10-8391-2010, 2010.
- Lehning, a, Zimmer, I., Steinbrecher, R., Brüggemann, N. and Schnitzler, J. P.: Isoprene synthase activity and its relation to isoprene emission in *Quercus robur* L. leaves, *Plant Cell Environ.*, 22(5), 495–504, doi:10.1046/j.1365-3040.1999.00425.x, 1999.
- Liu, J., D'Ambro, E. L., Lee, B. H., Lopez-Hilfiker, F. D., Zaveri, R. A., Rivera-Rios, J. C., Keutsch, F. N., Iyer, S., Kurten, T., Zhang, Z., Gold, A., Surratt, J. D., Shilling, J. E. and Thornton, J. A.: Efficient Isoprene Secondary Organic Aerosol Formation from a Non-IEPOX Pathway, *Environ. Sci. Technol.*, 50(18), 9872–9880, doi:10.1021/acs.est.6b01872, 2016.
- Nadzir, M. S. M., Cain, M., Robinson, A. D., Bolas, C., Harris, N. R. P., Parnikoza, I., Salimun, E., Mustafa, E. M., Alhasa, K. M., Zainuddin, M. H. M., Ghee, O. C., Morris, K., Khan, M. F., Latif, M. T., Wallis, B. M., Cheah, W., Zainudin, S. K., Yusop, N., Ahmad, M. R., Hussin, W. M. R. W., Salleh, S. M., Hamid, H. H. A., Lai, G. T., Uning, R., Bakar, M. A. A., Ariff, N. M., Tuah, Z., Wahab, M. I. A., Foong, S. Y., Samah, A. A., Chenoli, S. N., Wan Johari, W. L., Zain, C. R. C. M., Rahman,



- N. A., Rosenstiel, T. N., Yusoff, A. H., Sabuti, A. A., Alias, S. A. and Noor, A. Y. M.: Isoprene hotspots at the Western Coast of Antarctic Peninsula during MASEC'16, *Polar Sci.*, (May), 1–12, doi:10.1016/j.polar.2018.12.006, 2019.
- Nölscher, A. C., Yañez-Serrano, A. M., Wolff, S., de Araujo, A. C., Lavrič, J. V., Kesselmeier, J., Williams, J., Jlscher, A. C., Yañez-Serrano, A. M., Wolff, S., de Araujo, A. C., Lavrič, J. V., Kesselmeier, J. and Williams, J.: Unexpected seasonality in quantity and composition of Amazon rainforest air reactivity., *Nat. Commun.*, 7, 10383, doi:10.1038/ncomms10383, 2016.
- Otu-Larbi, F., Bolas, C. G., Ferracci, V., Staniaszek, Z., Jones, R. L., Malhi, Y., Harris, N. R. P., Wild, O. and Ashworth, K.: Modelling the effect of the 2018 summer heatwave and drought on isoprene emissions in a UK woodland, *Glob. Chang. Biol.*, gcb.14963, doi:10.1111/gcb.14963, 2019.
- Peters, R. and Bakkeren, H.: Sorbents in Sampling. Stability and Breakthrough Measurements, *Analyst*, 11(January), 71–74, 1994.
- Rhoderick, G. C., Cecelski, C. E., Miller, W. R., Worton, D. R., Moreno, S., Brewer, P. J., Viallon, J., Idrees, F., Moussay, P., Kim, Y. D., Kim, D., Lee, S., Baldan, A. and Li, J.: Stability of gaseous volatile organic compounds contained in gas cylinders with different internal wall treatments, *Elem Sci Anth*, 7(1), 28, doi:10.1525/elementa.366, 2019.
- Robinson, A. D., Millard, G. A., Danis, F., Guirlet, M., Harris, N. R. P., Lee, A. M., McIntyre, J. D., Pyle, J. A., Arvelius, J., Dagnesjo, S., Kirkwood, S., Nilsson, H., Toohey, D. W., Deshler, T., Goutail, F., Pommereau, J.-P., Elkins, J. W., Moore, F., Ray, E., Schmidt, U., Engel, A. and Müller, M.: Ozone loss derived from balloon-borne tracer measurements in the 1999/2000 Arctic winter, *Atmos. Chem. Phys.*, 5(5), 1423–1436, doi:10.5194/acp-5-1423-2005, 2005.
- Sharkey, T. D.: Is it useful to ask why plants emit isoprene?, *Plant, Cell Environ.*, 36(3), 517–520, doi:10.1111/pce.12038, 2013.
- Sharkey, T. D., Wiberley, A. E. and Donohue, A. R.: Isoprene emission from plants: Why and how, *Ann. Bot.*, 101(1), 5–18, doi:10.1093/aob/mcm240, 2008.
- Smith, I. M.: Software for Determining Polynomial Calibration Functions by Generalised Least Squares: User Manual, NPL Rep. MS11, Teddington, 2010.
- Squire, O. J., Archibald, A. T., Griffiths, P. T., Jenkin, M. E., Smith, D. and Pyle, J. A.: Influence of isoprene chemical mechanism on modelled changes in tropospheric ozone due to climate and land use over the 21st century, *Atmos. Chem. Phys.*, 15(9), 5123–5143, doi:10.5194/acp-15-5123-2015, 2015.
- Stone, D., Evans, M. J., Edwards, P. M., Commane, R., Ingham, T., Rickard, A. R., Brookes, D. M., Hopkins, J., Leigh, R. J., Lewis, A. C., Monks, P. S., Oram, D., Reeves, C. E., Stewart, D. and Heard, D. E.: Isoprene oxidation mechanisms: Measurements and modelling of OH and HO<sub>2</sub> over a South-East Asian tropical rainforest during the OP3 field campaign, *Atmos. Chem. Phys.*, 11(13), 6749–6771, doi:10.5194/acp-11-6749-2011, 2011.
- Visakorpi, K., Gripenberg, S., Malhi, Y., Bolas, C., Oliveras, I., Harris, N., Rifai, S. and Riutta, T.: Small-scale indirect plant responses to insect herbivory could have major impacts on canopy photosynthesis and isoprene emission, *New Phytol.*, 220(3), 799–810, doi:10.1111/nph.15338, 2018.
- Yañez-Serrano, A. M., Nölscher, A. C., Williams, J., Wolff, S., Alves, E., Martins, G. A., Bourtsoukidis, E., Brito, J., Jardine, K., Artaxo, P. and Kesselmeier, J.: Diel and seasonal changes of biogenic volatile organic compounds within and above an Amazonian rainforest, *Atmos. Chem. Phys.*, 15(6), 3359–3378, doi:10.5194/acp-15-3359-2015, 2015.